



# Treball Final de Grau

**Numerical simulation study on the temperature dependence of the Arrhenius parameters and its relation with the kinetic compensation effect**

**Estudi per simulacions numèriques de la dependència amb la temperatura dels paràmetres d'Arrhenius i la seva relació amb l'efecte de compensació cinètic**

Iker Albuquerque Alvarez

*January 2020*



UNIVERSITAT DE  
BARCELONA

**B:KC** Barcelona  
Knowledge  
Campus  
Campus d'Excel·lència Internacional



Aquesta obra està subjecta a la llicència de:  
Reconeixement–NoComercial–SenseObraDerivada



<http://creativecommons.org/licenses/by-nc-nd/3.0/es/>



*If you spend any time spinning hypotheses, checking to see whether they make sense, whether they conform to what else we know, thinking of tests you can pose to substantiate or deflate hypotheses, you will find yourself doing science.*

Carl Sagan

First of all, I would like to show my gratitude to Dr. Joaquín F. Pérez de Benito for being the best guide I could have had through my degree final project. His scientific support, patience and analysis abilities are worth to be remembered.

Thanks are due also to my parents and girlfriend for their emotional support and unconditional confidence during the development of the present work, highs and lows included, as well as in every other aspect of my life.



**REPORT**





# CONTENTS

<b>1. SUMMARY</b>	3
<b>2. RESUM</b>	5
<b>3. INTRODUCTION</b>	7
<b>4. OBJECTIVES</b>	8
<b>5. METHODS AND CALCULATIONS</b>	9
5.1. Random-number generator	9
5.2. Calculations and graphics	10
<b>6. TEMPERATURE DEPENDENCE OF THE ACTIVATION PARAMETERS</b>	10
6.1. Arrhenius equation: the original law and its modified version	10
6.2. Eyring equation: the original law and its modified version	11
<b>7. COMPENSATION EFFECT: ISOKINETIC TEMPERATURE</b>	12
7.1. Activation energy vs. pre-exponential factor linear correlation	12
7.2. Activation enthalpy vs. activation entropy linear correlation	13
<b>8. NUMERICAL SIMULATIONS</b>	14
8.1. A new physical model: conditions of linearity	14
8.2. Isokinetic temperature: discounting the effect of random errors	19
<b>9. APPLICATION TO BIBLIOGRAPHIC DATA</b>	29
9.1. Physical model: doubling temperature values	29
9.2. Seeking the true isokinetic temperature: highest probability values	32
<b>10. CONCLUSIONS</b>	37
<b>11. REFERENCES</b>	38
<b>APPENDICES</b>	41
Appendix 1: Statistical methods	43
Appendix 2: Theoretical background: general model	44
Appendix 3: Application to chemical kinetics: modified Eyring law	48
Appendix 4: Tabulated kinetic data	49



## 1. SUMMARY

The original version of the Arrhenius equation does not take into account the temperature dependence of both the pre-exponential factor and the activation energy. However, a simple physical argument makes clear that this hypothesis (although valid indeed as an approximation) is not totally accurate. The two Arrhenius parameters are mutually interconnected, so that an increase of one of them with temperature leads to an increase of the other. This might be taken as a potential explanation of the widespread compensation effect, and the conditions under which this model results applicable have been explored by means of numerical simulations. An interesting parameter involved in them is  $T_d$ , the temperature corresponding to an activation energy that exactly doubles the value at 0 K. Provided that this magnitude does not differ much from one member of a homologous reaction series to another, there will be a linear  $E_a$  vs.  $R \ln A$  ( or  $\Delta H_{\ddagger}^{\circ}$  vs.  $\Delta S_{\ddagger}^{\circ}$  ) relationship, its slope being the isokinetic temperature,  $T_{ik}$  (when  $T = T_{ik}$  all the reactions of the series share the same rate constant). This physical model seems to be supported by the low values of parameter  $T_d$  obtained for chemical reactions involving proteins as reactants. Additionally, given that the random experimental errors provoke a shift in parameter  $T_{ik}$  toward the mean working temperature, this effect has been discounted in order to obtain the most probable (extrapolated) value of the isokinetic temperature for different reaction families selected from chemical bibliographic sources.

**Keywords:** isokinetic temperature, kinetic compensation effect, modified Arrhenius and Eyring equations, numerical simulations, temperature-dependent activation energy.



## 2. RESUM

La versió original de l'equació d'Arrhenius no té en compte les dependències amb la temperatura tant del factor pre-exponencial com de l'energia d'activació. Malgrat això, un simple argument físic deixa ben clar que aquesta hipòtesi (tot i que vàlida com una aproximació) no es del tot acurada. Els dos paràmetres d'Arrhenius estan mútuament interconnectats, de manera que un augment d'un amb la temperatura causa un augment de l'altre. Aquest fet es pot prendre com a una potencial explicació del efecte de compensació àmpliament estès, i les condicions sota les quals aquest model pot aplicar-se s'han explorat mitjançant simulacions numèriques. Un paràmetre interessant implicat en elles es  $T_d$ , la temperatura a la qual el valor de l'energia d'activació es exactament el doble del que tindria a 0 K. Sempre que aquesta magnitud no varii massa entre els membres d'una mateixa família de reaccions homòlogues, hi haurà una correlació lineal entre  $E_a$  i  $R \ln A$  (o entre  $\Delta H_{\ddagger}^{\circ}$  i  $\Delta S_{\ddagger}^{\circ}$ ), sent el pendent igual a la temperatura isocinètica,  $T_{ik}$  (quan  $T = T_{ik}$  totes les reaccions de la sèrie tenen la mateixa constant de velocitat). Aquest model físic sembla ser recolzat pels valors baixos del paràmetre  $T_d$  obtinguts a partir de reaccions químiques involucrant proteïnes com a reactius. A més, com que els errors aleatoris experimentals provoquen un canvi al paràmetre  $T_{ik}$  que fa que tendeixi cap a la temperatura mitjana de treball, s'ha descomptat aquest efecte amb la intenció d'obtenir la temperatura isocinètica més probable (extrapolada) per a diferents famílies de reaccions extretes de fonts bibliogràfiques.

**Paraules clau:** efecte de compensació cinètic, energia d'activació dependent de la temperatura, equacions modificades d'Arrhenius i Eyring, simulacions numèriques, temperatura isocinètica.

..



### 3. INTRODUCTION

Most chemical kineticists are familiar with the linear relationships involving either the Arrhenius ( $E_a$  vs.  $\ln A$ ) or Eyring ( $\Delta H_{\ddagger}^0$  vs.  $\Delta S_{\ddagger}^0$ ) parameters found in the study of many homologous reaction series. Such a striking behavior has been known at least from 1925,<sup>1</sup> and it has been reported time and time again in scientific papers since then.<sup>2-5</sup>

However, this kind of correlations is by no means restricted to the field of chemical kinetics, since it can also be found when handling equations of the general type:

$$Y_T = Y_{\infty} e^{-\frac{X}{RT}} \quad (1)$$

corresponding to thermally activated processes, where  $Y_T$  and  $Y_{\infty}$  are the values of a temperature-dependent physicochemical magnitude at the absolute temperatures  $T$  and  $\infty$ , respectively,  $X$  is the energy barrier and  $R$  the ideal gas constant. Quite often, when the experimental  $X$  data are plotted against  $\ln Y_{\infty}$  for a series of closely related processes, a positive-slope linear relationship is found:

$$X_i = X_h + RT_{\text{iso}} \ln Y_{\infty,i} \quad (2)$$

where  $X_i$  and  $Y_{\infty,i}$  are the parameters corresponding to a particular member of the series  $i$ ,  $X_h$  is the value of  $X$  for a hypothetical member with  $\ln Y_{\infty} = 0$  and  $T_{\text{iso}}$  is the temperature at which all the members of the series share the same value of the physicochemical magnitude under study (compensation effect), its natural logarithm being (from eqs 1 and 2):

$$\ln Y_{T_{\text{iso}}} = -\frac{X_h}{RT_{\text{iso}}} \quad (3)$$

This situation appears in a wide variety of physicochemical phenomena, the magnitude  $Y_T$  adopting alternatively the form of: a rate constant (Arrhenius equation);<sup>6</sup> a rate constant/temperature ratio (Eyring equation);<sup>7,8</sup> a reaction equilibrium constant (van't Hoff equation);<sup>9</sup> an adsorption equilibrium constant;<sup>10</sup> an  $\alpha/(1-\alpha)$  ratio ( $\alpha$  being the mass accommodation coefficient in the absorption of gas molecules by liquids);<sup>11,12</sup> a viscous liquid fluidity;<sup>13</sup> a diffusion coefficient;<sup>14-16</sup> a polymer relaxation frequency;<sup>17</sup> an annealing rate of

metastable defects;<sup>18</sup> a rate of crystal growth;<sup>19</sup> a thermal electron emission rate from semiconductor traps;<sup>20</sup> or a solid-state electrical conductivity.<sup>21-25</sup>

As pointed out by other authors,<sup>26</sup> the widespread occurrence of this compensation effect in quite different kinds of phenomena (covering not only the above mentioned fields of chemistry and physics but also that of food technology<sup>27</sup>) seems to claim for a common explanation. Actually, the influence that both random<sup>28-31</sup> and systematic<sup>32</sup> errors in the experimental data might have on the observation of the compensation effect has been conveniently explored. In order to fill a still existing gap, the present contribution will be committed to analyze the potential impact that an error, not coming properly from the experiments performed, but rather from the mathematical model used to fit the experimental data (i.e., the temperature dependence of parameters  $Y_\infty$  and  $X$  appearing in eq 1), might have on the occurrence of the compensation plots, placing a special focus on the field of chemical kinetics (Arrhenius and Eyring equations).

## 4. OBJECTIVES

Three different objectives will be considered in this project:

*First: Deducing the modified Arrhenius and Eyring equations.* Among the things one should keep in mind when approaching to science, and particularly so in the field of physical chemistry, stands out the realization that all mathematical models are only approximations to the real behavior of nature. Relevant to the specific purpose of the present study is the fact that the temperature dependence of the rate constants, as described by both the Arrhenius and Eyring equations, does not take into consideration that the pre-exponential factor and the activation energy on one side, and the activation enthalpy and entropy on the other, are all four actually dependent on the temperature used in the experiments. This work will start with the integration of the differential forms of the Arrhenius and Eyring equations, once included the temperature dependence of the activation parameters, to obtain the modified versions of those laws.

*Second: Finding the conditions for a compensation effect.* Once the development of the modified Arrhenius and Eyring equations is completed, numerical simulations will be performed in order to know under which conditions those laws are able to explain the existence of a kinetic compensation effect. In particular, different temperature dependences of the activation energy,



varying either systematically or randomly from one reaction of the homologous series to another, will be analyzed with this end in view.

*Third: Searching for the real isokinetic temperature value.* This research project will finish with a numerical simulation study of the effect that accidental errors exert on the value of the slope of the linear compensation plot, using real experimental cases taken from the chemical literature, and thus obtaining the most probable value of the parameter known as isokinetic temperature of the reaction series (at which all the members have in common the same rate constant).

The rationale for the present work can be summarized in the following question: Is the temperature dependence of the activation parameters capable of explaining at least some of the kinetic compensation plots observed in the laboratory? The answer to this problem will be sought by computer calculations and presented hereafter.

## 5. METHODS AND CALCULATIONS

### 5.1. RANDOM-NUMBER GENERATOR

In some of the programs needed to perform the numerical calculations involved in the present study a set of scattered numbers was required (for instance, to simulate the accidental errors associated with all experimental measurements). In order to achieve this, a random number generator was included in one of the subroutines of the different programs, starting with the square root  $\sqrt{J-n}$ , where  $J$  changed from one simulation to another and took either integer or non-integer values indifferently,  $n$  being a fixed non-integer number (to avoid the occurrence of perfect squares). The scattered values were taken from the successive decimal digits of the corresponding square roots, and a random positive or negative sign was ascribed depending on the nature of the first digit (even or odd). Afterwards, these arrays of random numbers were used as required, the main application being the simulation of the accidental errors associated with the experimental determination of the rate constants at different temperatures.

## 5.2. CALCULATIONS AND GRAPHICS

When necessary, linear fits were performed by means of the least square method (see Appendix 1).<sup>33</sup> The hardware used in all the numerical simulations and figures was a Sony Vaio personal computer, and the software employed for the calculations was the programming language BBC BASIC (version for Windows) and for the graphics the program KaleidaGraph (version 4.03).

## 6. TEMPERATURE DEPENDENCE OF THE ACTIVATION PARAMETERS

With the purpose of seeking a new explanation of the compensation effect (either kinetic or belonging to other fields of physics and chemistry), it has been taken into consideration the dependence (assumed to be linear for the sake of simplicity) of parameter  $X$  in eq 1 on temperature.<sup>34-37</sup> By integration of the corresponding differential equation (see Appendix 2), it follows that:

$$Y_T = A_X T^{\frac{X_0}{RT_d}} e^{-\frac{X_0}{RT}} \quad (4)$$

where parameter  $A_X$  is the new pre-exponential factor,  $X_0$  the activation barrier at 0 K and  $T_d$  the doubling temperature (at which  $X = 2 X_0$ ).

### 6.1. ARRHENIUS EQUATION: THE ORIGINAL LAW AND ITS MODIFIED VERSION

The dependence of the rate constant of a chemical reaction on the absolute temperature can be expressed by means of the Arrhenius equation:

$$k_T = A e^{-\frac{E_a}{RT}} \quad (5)$$

where  $A$  is the pre-exponential factor and  $E_a$  the activation energy of the reaction under consideration.

However, eq 11-A (developed in Appendix 2 for a general phenomenon incorporating an activation barrier) can be written in the case of chemical kinetics as the modified Arrhenius equation:

$$k_T = A_E T^{\frac{E_{a,o}}{RT_d}} e^{-\frac{E_{a,o}}{RT}} \quad (6)$$

where  $E_{a,o}$  is the activation energy at 0 K for each member of the reaction series,  $T_d$  the doubling temperature (at which  $E_{a,T} = 2E_{a,o}$ ) and parameter  $A_E$  comes from the integration constant, its physical significance being that of the value (independent of temperature) the rate constant would take for a hypothetical non-activated process with  $E_{a,o} = 0$ .

Equation 6 has been reported to accommodate the experimental kinetic data better than the original Arrhenius law (a particular case of the modified version with  $T_d = \infty$ ).<sup>38-40</sup> Other modifications of this equation have been proposed for special situations, for instance to fit the experimental rate constants obtained at very low temperatures.<sup>41</sup>

## 6.2. EYRING EQUATION: THE ORIGINAL LAW AND ITS MODIFIED VERSION

According to the transition state theory, the dependence of the rate constant on the absolute temperature can be expressed by means of the Eyring equation:

$$k_T = \frac{k_B T}{h} (c^\circ)^{1-n} e^{\frac{\Delta S_\ddagger^\circ}{R}} e^{-\frac{\Delta H_\ddagger^\circ}{RT}} \quad (7)$$

thus representing an alternative to the Arrhenius law,  $k_B$  and  $h$  being the Boltzmann and Planck constants, respectively,  $c^\circ$  the standard concentration (to guarantee the dimensional homogeneity of the equation<sup>42</sup>),  $n$  the kinetic order,  $\Delta S_\ddagger^\circ$  the activation entropy and  $\Delta H_\ddagger^\circ$  the activation enthalpy.

However, taking into consideration the temperature dependence of the activation enthalpy, a simple mathematical argument (see Appendix 3) leads to the modified Eyring equation:

$$k_T = A_H T^{1 + \frac{\Delta H_{\ddagger,o}^\circ}{RT_d}} e^{-\frac{\Delta H_{\ddagger,o}^\circ}{RT}} \quad (8)$$

where  $\Delta H_{\ddagger,o}^\circ$  is the activation enthalpy at 0 K for each member of the reaction series,  $T_d$  is the doubling temperature (at which  $\Delta H_{\ddagger,T}^\circ = 2\Delta H_{\ddagger,o}^\circ$ ) and parameter  $A_H$  comes from the new

integration constant, its physical significance being now that of the value (independent of temperature) the rate constant/temperature ratio would take for a hypothetical process with  $\Delta H_{\neq,0}^{\circ} = 0$ .

## 7. COMPENSATION EFFECT: ISOKINETIC TEMPERATURE

### 7.1. ACTIVATION ENERGY VS. PRE-EXPONENTIAL FACTOR LINEAR CORRELATION

As pointed out before, the experimental data found for many activated physical and chemical phenomena follow compensation laws of the type shown in eq 2. When the magnitude determined is a reaction rate constant and the law involved the Arrhenius equation, the correlation can be written as:

$$E_{a,i} = E_{a,h} + R T_{ik} \ln A_i \quad (9)$$

where  $E_{a,i}$  and  $A_i$  are the Arrhenius parameters corresponding to a particular member of the homologous series,  $E_{a,h}$  is the value of the activation energy for a hypothetical reaction with  $\ln A_i = 0$  and  $T_{ik}$  is the isokinetic temperature. When  $T = T_{ik}$  all the members of the series share the same value of the rate constant, its natural logarithm being (from eqs 5 and 9):

$$\ln k_{T_{ik}} = - \frac{E_{a,h}}{RT_{ik}} \quad (10)$$

The reason for talking of the existence of a kinetic compensation effect lies in the observational fact that for many families of related chemical reactions an increase in the activation energy (unfavorable to the reaction rate) is found to be associated with another increase in the pre-exponential factor (favorable to the reaction rate), the compensation being total when the experimental temperature equals the  $T_{ik}$  value.

As a real case example taken from the chemical literature, let us consider the kinetic behavior of the air oxidation of Fe(II) complexes with biologically active tridentate pyridyl

thiosemicarbazone ligands in methanol solutions,<sup>43</sup> for which a linear compensation plot in the activation energy vs. pre-exponential factor plane can be observed (Figure 1, left), yielding an isokinetic temperature of  $440 \pm 25$  K (well above the working temperature range).

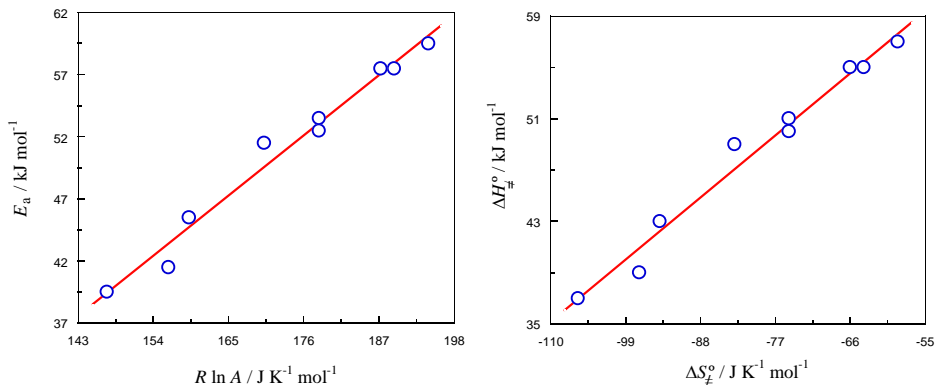


Figure 1. Kinetic compensation plots derived from Arrhenius (left) and Eyring (right) data for the air oxidation of Fe(II) complexes with biologically active tridentate pyridyl thiosemicarbazone ligands in methanol solutions.

## 7.2. ACTIVATION ENTHALPY VS. ACTIVATION ENTROPY LINEAR CORRELATION

If the temperature - rate constant data are fitted to the Eyring equation, the compensation correlations (when applicable) are of the type:

$$\Delta H_{\neq,i}^{\circ} = \Delta H_{\neq,h}^{\circ} + T_{\text{ik}} \Delta S_{\neq,i}^{\circ} \quad (11)$$

where  $\Delta H_{\neq,i}^{\circ}$  and  $\Delta S_{\neq,i}^{\circ}$  are the activation enthalpy and entropy, respectively, for a particular member of the homologous series,  $\Delta H_{\neq,h}^{\circ}$  is the value of the activation enthalpy for a hypothetical reaction with  $\Delta S_{\neq,i}^{\circ} = 0$ .

From eqs 7 and 11 it follows that, if the experimental temperature equals the isokinetic one ( $T = T_{\text{ik}}$ ), the reactions belonging to the considered family would show the rate constant:

$$k_{\text{iso}} = \frac{k_{\text{B}} T_{\text{ik}}}{h} (c^{\circ})^{1-n} e^{-\frac{\Delta H_{\neq,h}^{\circ}}{RT_{\text{ik}}}} \quad (12)$$

and this value would be the same indeed for all the chemical processes of the series, since the intercept ( $\Delta H_{\neq, h}^{\circ}$ ) and slope ( $T_{ik}$ ) of the linear compensation plot remain invariable throughout the reaction family.

A representative case of this kind of behavior corresponding to the homologous series mentioned above [air oxidation of Fe(II) complexes] is displayed in Figure 1, right, leading to an identical isokinetic temperature ( $440 \pm 25$  K).

## 8. NUMERICAL SIMULATIONS

### 8.1. A NEW PHYSICAL MODEL: CONDITIONS OF LINEARITY

Equation 6 by itself cannot explain the existence of an  $E_a - \ln A$  kinetic compensation effect unless a different value of the exponent  $E_{a,o}/RT_d$  corresponds to each member of the homologous reaction series ( $T_d$  must not be directly proportional to  $E_{a,o}$ ). Hence, given its mathematical structure, eq 6 implies the existence of a certain correlation between the Arrhenius pre-exponential factor and the activation energy for a homologous reaction series provided that the doubling temperature ( $T_d$ ) is not directly proportional to the activation energy at 0 K ( $E_{a,o}$ ) for each member of the series (since, in that case, the correlation would vanish).

Thus, as a particular case of eq 14-A (see Appendix 2), for a homologous reaction series it could be written:

$$E_{a,i} = R \frac{T_m + T_d}{1 + \ln T_m} \ln \frac{A_i}{A_E} \quad (13)$$

yielding a linear relationship in an  $E_a - \ln A$  plane provided that parameters  $T_m$ ,  $T_d$  and  $A_E$  take the same values (or at least very similar) for all the members of the series.

In order to analyze the conditions required for eq 6 to explain the kinetic compensation effect, it has been assumed that there is a simple linear dependence of both parameters  $T_d$  and  $A_E$  on the activation energy at 0 K corresponding to each member of the reaction homologous series:

$$T_d = T_{d,o} + \frac{dT_d}{dE_{a,o}} E_{a,o} \quad (14)$$

$$A_E = A_{E,o} + \frac{dA_E}{dE_{a,o}} E_{a,o} \quad (15)$$

where  $T_{d,o}$  and  $A_{E,o}$  are the values of parameters  $T_d$  and  $A_E$ , respectively, for a hypothetical member of the reaction series with  $E_{a,o} = 0$ .

When the activation energy  $E_a$  was plotted against the logarithm of the Arrhenius pre-exponential factor, a change in  $dT_d/dE_{a,o}$  (with fixed values of the other three parameters:  $T_{d,o}$ ,  $A_{E,o}$  and  $dA_E/dE_{a,o}$ ) led either to a perfect straight line ( $dT_d/dE_{a,o} = 0$ ), to downward-concave curves ( $dT_d/dE_{a,o} < 0$ ) or to upward-concave curves ( $dT_d/dE_{a,o} > 0$ ) (Figure 2, left). For a fixed value of  $dT_d/dE_{a,o} > 0$ , an increase in parameter  $T_{d,o}$  led to plots losing their upward-concave curvature and getting closer and closer to a perfect straight line (reaching asymptotically that limit at  $T_{d,o} = \infty$ ) (Figure 3, left). A change in  $dA_E/dE_{a,o}$  led either to a perfect straight line ( $dA_E/dE_{a,o} = 0$ ) or to upward-concave curves ( $dA_E/dE_{a,o} > 0$ ) (Figure 4, left), whereas a change in  $A_{E,o}$  led to upward-concave curves that gradually lost their curvature as that parameter increased (Figure 5, left).

Nevertheless, when the  $E_a - \ln A$  data were fitted to straight lines, those plots yielded acceptable linear correlation coefficients ( $r \geq 0.990$ ) in 23 out of 34 cases (Figures 2 and 3, right; Figures 4 and 5, right, filled circles). It is noteworthy, however, that when the  $E_a = 0$  point was excluded from the  $E_a - \ln A$  correlations with variable  $dA_E/dE_{a,o}$ , almost perfectly linear plots ( $r \geq 0.9995$ ) were obtained in all the 15 cases considered (empty circles in Figures 4 and 5, right).

On the other hand, provided that  $dT_d/dE_{a,o} = 0$ , the  $E_a - \ln A$  plots were linear when parameter  $A_E$  took random values for the different members of the homologous series (Figure 6, left), the linear correlation coefficient decreasing as the doubling temperature  $T_{d,o}$  increased (Figure 6, right). Moreover, provided that  $dB/dE_{a,o} = 0$ , the  $E_a - \ln A$  plots were also linear when parameter  $T_{d,o}$  took random values (within a  $\pm 10\%$  range) for the members of the series (Figure 7,  $r \geq 0.991$ ).

For a homologous reaction series it follows [from eqs 7, 21-A and 24-A (Appendix 3)] that:

$$\Delta H_{\neq,i}^{\circ} = \frac{T_m + T_d}{1 + \ln T_m} \left[ R \ln \frac{k_B (c^{\circ})^{1-n}}{h A_H} + \Delta S_{\neq,i}^{\circ} \right] \quad (16)$$

yielding now a linear relationship in the enthalpy-entropy plane provided that parameters  $T_m$ ,  $T_d$  and  $A_H$  are the same (or at least very similar) for all the members of the series.

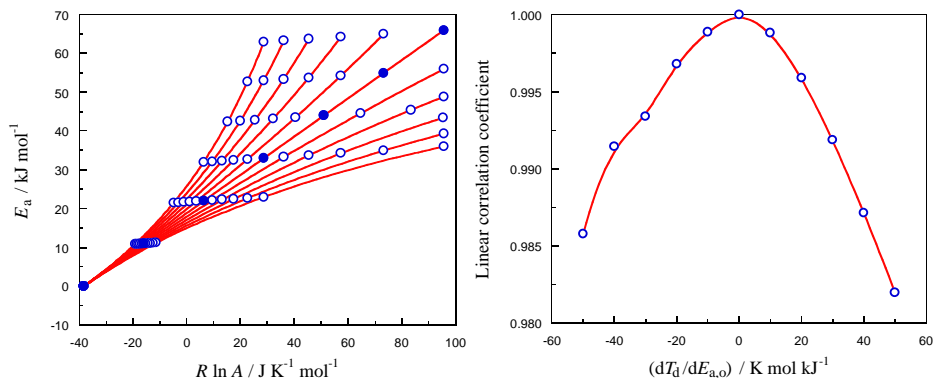


Figure 2. Results from numerical simulations performed over the temperature range 15.0 – 35.0 °C with  $E_{a,0} = 0 - 60 \text{ kJ mol}^{-1}$ ,  $A_{E,0} = 10^{-2} \text{ rcu}$ ,  $dA_E/dE_{a,0} = 0$  and  $T_{d,0} = 3 \times 10^3 \text{ K}$  (rcu stands for rate constant units). Left: activation energy as a function of the logarithm of the Arrhenius pre-exponential factor at  $dT_d/dE_{a,0} = -50, -40, -30, -20, -10, 0, 10, 20, 30, 40$  and  $50$  (from right to left)  $\text{K mol kJ}^{-1}$ ; the perfectly linear  $E - \ln A$  correlation ( $dT_d/dE_{a,0} = 0$ ) is indicated by solid circles. Right: linear correlation coefficient of the  $E_a - \ln A$  plots as a function of  $dT_d/dE_{a,0}$ .

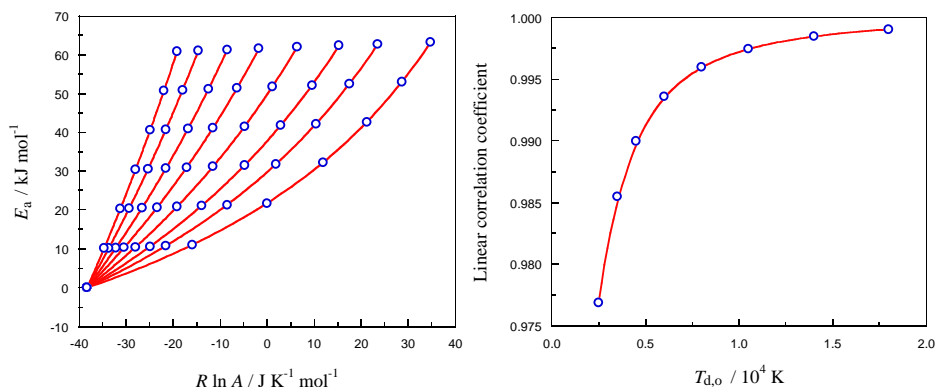


Figure 3. Results from numerical simulations performed over the temperature range 15.0 – 35.0 °C with  $E_{a,0} = 0 - 60 \text{ kJ mol}^{-1}$ ,  $A_{E,0} = 10^{-2} \text{ rcu}$ ,  $dA_E/dE_{a,0} = 0$  and  $dT_d/dE_{a,0} = 50 \text{ K mol kJ}^{-1}$  (rcu stands for rate constant units). Left: activation energy as a function of the logarithm of the Arrhenius pre-exponential factor at  $T_{d,0} = 0.25, 0.35, 0.45, 0.60, 0.80, 1.05, 1.40$  and  $1.80$  (from right to left)  $\times 10^4 \text{ K}$ . Right: linear correlation coefficient of the  $E_a - \ln A$  plots as a function of parameter  $T_{d,0}$ .



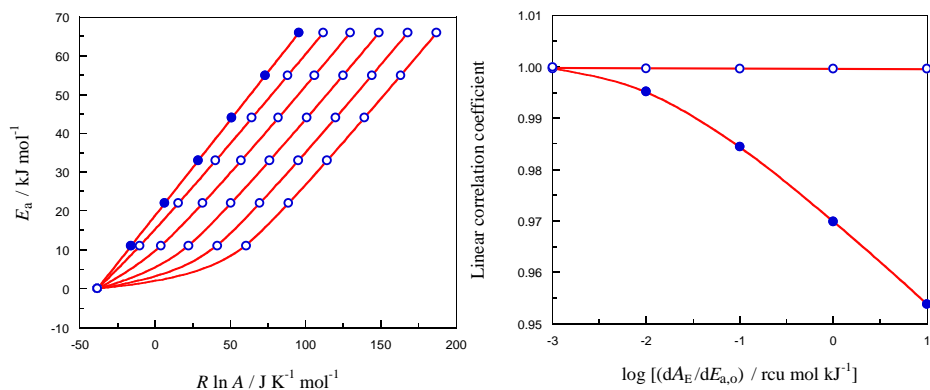


Figure 4. Results from numerical simulations performed over the temperature range 15.0 – 35.0 °C with  $E_{a,0} = 0 - 60 \text{ kJ mol}^{-1}$ ,  $A_{E,0} = 10^{-2} \text{ rcu}$ ,  $T_{d,0} = 3 \times 10^3 \text{ K}$  and  $dT_d/dE_{a,0} = 0$  (rcu stands for rate constant units). Left: activation energy as a function of the logarithm of the Arrhenius pre-exponential factor at  $dA_E/dE_{a,0} = 0, 0.001, 0.01, 0.1, 1$  and 10 (from left to right)  $\text{rcu mol kJ}^{-1}$ ; the perfectly linear  $E_a - \ln A$  correlation ( $dA_E/dE_{a,0} = 0$ ) is indicated by solid circles. Right: linear correlation coefficient of the  $E_a - \ln A$  plots as a function of the logarithm of  $dA_E/dE_{a,0}$ ; filled circles: all points included in the correlation; empty circles: the  $E_a = 0$  point excluded from the correlation.

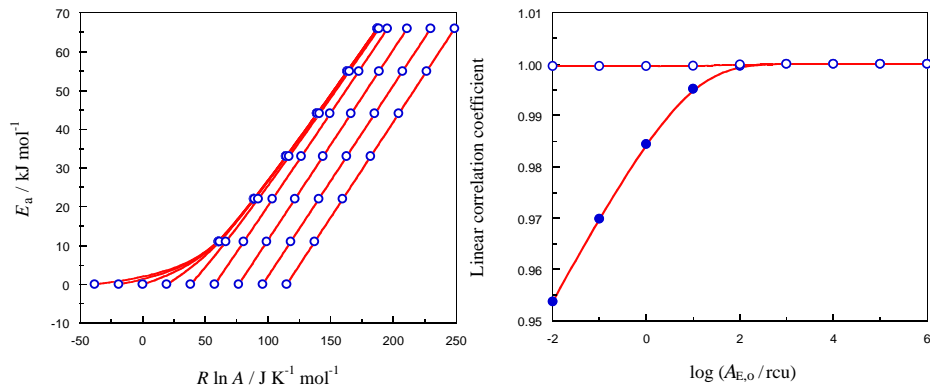


Figure 5. Results from numerical simulations performed over the temperature range 15.0 – 35.0 °C with  $E_{a,0} = 0 - 60 \text{ kJ mol}^{-1}$ ,  $dA_E/dE_{a,0} = 10 \text{ rcu mol kJ}^{-1}$ ,  $T_{d,0} = 3 \times 10^3 \text{ K}$  and  $dT_d/dE_{a,0} = 0$  (rcu stands for rate constant units). Left: activation energy as a function of the logarithm of the Arrhenius pre-exponential factor at  $\log (A_{E,0}/\text{rcu}) = -2, -1, 0, 1, 2, 3, 4, 5$  and 6 (from left to right). Right: linear correlation coefficient of the  $E_a - \ln A$  plots as a function of  $\log A_{E,0}$ ; filled circles: all points included in the correlation; empty circles: the  $E_a = 0$  point excluded from the correlation.

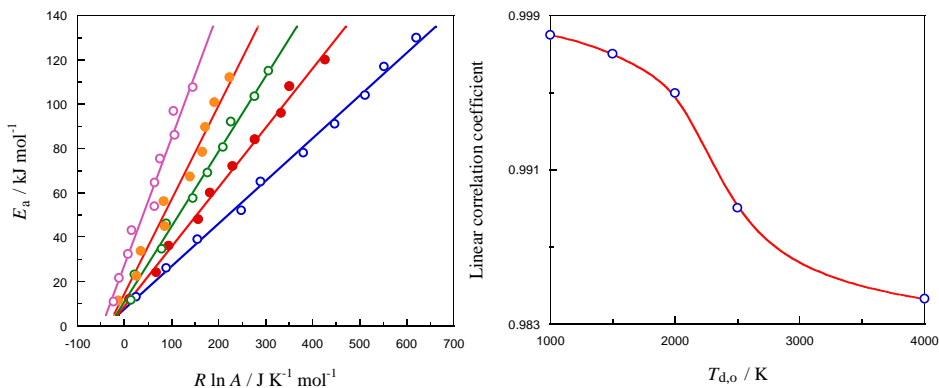


Figure 6. Results from numerical simulations performed over the temperature range 15.0 – 35.0 °C with  $E_{a,o} = 10 - 100 \text{ kJ mol}^{-1}$ ,  $A_{E,o} = 0.001 - 0.100$  (random values) rcu,  $dA_E/dE_{a,o} = 0$  and  $dT_d/dE_{a,o} = 0$  (rcu stands for rate constant units). Left: activation energy as a function of the logarithm of the Arrhenius pre-exponential factor at  $T_{d,o} = 1.0, 1.5, 2.0, 2.5$  and  $4.0$  (from right to left)  $\times 10^3$  K. Right: linear correlation coefficient of the  $E_a - \ln A$  plots as a function of parameter  $T_{d,o}$ .

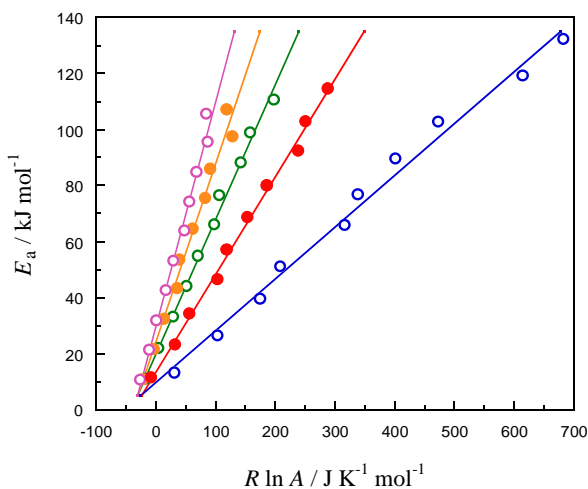


Figure 7. Activation energy as a function of the logarithm of the Arrhenius pre-exponential factor from numerical simulations performed over the temperature range 15.0 – 35.0 °C at random doubling temperatures within  $\pm 10\%$  of the average values  $T_{d,o} = 1, 2, 3, 4$  and  $5$  (from right to left)  $\times 10^3$  K with  $E_{a,o} = 10 - 100 \text{ kJ mol}^{-1}$ ,  $A_{E,o} = 1.00 \times 10^{-2}$  rcu,  $dA_E/dE_{a,o} = 0$  and  $dT_d/dE_{a,o} = 0$  (rcu stands for rate constant units)

## 8.2. ISOKINETIC TEMPERATURE: DISCOUNTING THE EFFECT OF RANDOM ERRORS

Permanganate is extensively used as a versatile oxidizing agent in the chemistry laboratory.<sup>44-47</sup> However, whereas potassium permanganate is soluble in water, most organic substrates are only soluble in low polarity organic solvents. This limitation can be overcome by the use of the compounds known as phase transfer agents, such as crown ethers or quaternary ammonium salts.<sup>48</sup> In particular, for the oxidation of a series of substituted cinnamic acids by tributylmethylammonium permanganate in methylene chloride solutions, it has been found the occurrence of a kinetic compensation effect especially interesting because the reported isokinetic temperature ( $627 \pm 52$  K) is much higher than the mean experimental one (286 K),<sup>49,50</sup> thus minimizing the probability that the observed correlation might be caused by the accumulation of random experimental errors rather than by a real physical phenomenon.<sup>51-57</sup>

In order to implement the numerical simulations, the following steps were carried out: i) First of all, the values of the activation enthalpies (ordinates) corresponding to a perfect linear relationship with the same intercept and slope as those of the compensation plot found in the laboratory (and reported in the bibliographic source) were calculated, all the while keeping invariant the experimental activation entropies (abscissas). ii) Then, the theoretical rate constants at different temperatures were obtained for each member of the reaction series using the Eyring equation. iii) Afterwards, the accidental errors of the rate constants for each member of the reaction series were incorporated into the simulations by means of a random-number generator, leading to a cloud of scattered theoretical points. iv) Finally, the simulated activation parameters were inferred making use again of the Eyring equation, leading to a new enthalpy-entropy correlation to be compared with the experimental one.

When the simulations were performed taking as a basis the above-mentioned homologous series corresponding to the permanganate oxidation of substituted cinnamic acids, it was observed that, as the maximum limit allowed for the accidental errors increased from 0 to 100 %, the correlation coefficient of the compensation plot first decreased, passed through a minimum and then increased to approach asymptotically the unity value associated with a perfect straight line (Figure 8, left). At the same time, the slope decreased from the experimental isokinetic temperature to scattered data close to the mean working temperature (Figure 8, right).

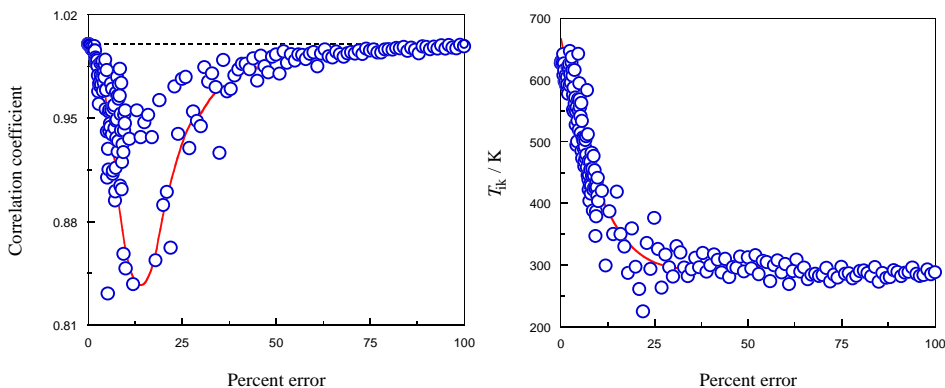


Figure 8. Correlation coefficient (left) and isokinetic temperature (right) as a function of the maximum limit allowed to the percent random errors of the rate constants for the simulated compensation plots based on the oxidation of a series of substituted cinnamic acids by tributylmethylammonium permanganate in methylene chloride solutions, assuming that in the absence of errors there exists a perfect enthalpy-entropy straight line with a slope equal to the experimental isokinetic temperature (627 K). The dashed line corresponds to a perfect enthalpy-entropy correlation ( $r = 1$ ).

The fitting error associated with the compensation plot was defined from the absolute values of the deviations of the experimental activation enthalpies with respect to the best adjusting straight line as obtained by means of the least square method:

$$E = \frac{\sum_{i=1}^N \left| \Delta H_{\neq,i,\text{exp}}^{\circ} - \Delta H_{\neq,i,\text{cal}}^{\circ} \right|}{N} \quad (17)$$

where  $\Delta H_{\neq,i,\text{exp}}^{\circ}$  and  $\Delta H_{\neq,i,\text{cal}}^{\circ}$  are the experimental and calculated values of the activation enthalpy for each member of the homologous series, respectively, and  $N$  is the total number of reactions studied.

The experimental point was placed on a  $T_{\text{ik}}$  vs.  $E$  diagram (Figure 9, left). In the case under study, the point was characterized by the coordinates ( $T_{\text{ik}} = 627 \text{ K}$ ,  $E = 0.75 \text{ kJ mol}^{-1}$ ) on that plane. Then, the scattered simulation points were added to the plot, obtained each of them from a set of reactions whose number equaled that of the experimental homologous series ( $N = 13$ ). Finally, the maximum probability curve for the ( $T_{\text{ik}}$ ,  $E$ ) couples could be drawn taking this time as a starting point for the simulations a set of  $10^5$  reactions. Actually, the perfect maximum probability curve would require a family with an infinite number of reactions but, because of the

material impossibility to implement this condition, a finite ensemble with a high number of reactions was accepted as a good enough approximation.

It is interesting to highlight as a result of this numerical study that, when the magnitude of the accidental errors increased, the slope of the compensation plot gradually decreased, showing a trend to approach the mean experimental temperature if the errors were high enough, thus going from a hypothesized perfect linear correlation ( $r = 1$ ) with a slope equal to the experimental isokinetic temperature ( $T_{ik}$ ) to an almost perfect straight line ( $r > 0.990$ ) with a slope equal to the mean working temperature ( $T_m$ ).

In order to find the highest probability value of the isokinetic temperature, the slope of the assumed perfect enthalpy-entropy straight line was systematically changed (by means of a computer program developed for that purpose) until achieving a situation where the experimental point exactly matched one of those belonging to the maximum probability curve. That happened when the slope of the assumed isokinetic plot was 681 K (Figure 9, right).

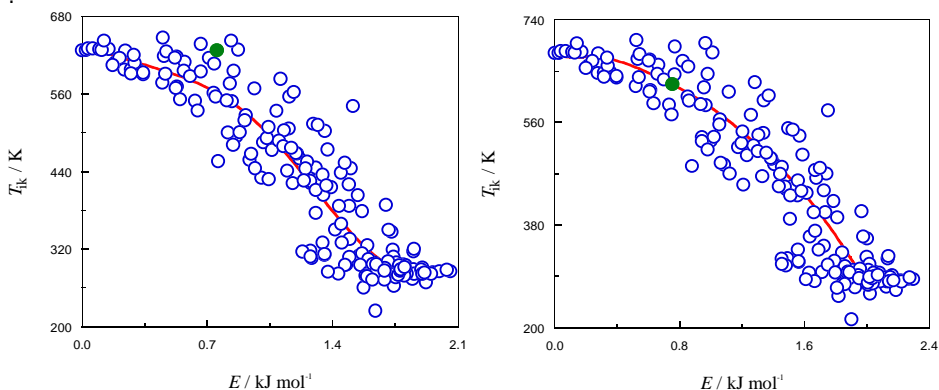


Figure 9. Isokinetic temperature as a function of the fitting error for the simulated enthalpy-entropy compensation plots based on the oxidation of a series of substituted cinnamic acids by tributylmethylammonium permanganate in methylene chloride solutions, showing the experimental point (filled circle), the points obtained from computer simulations incorporating accidental errors (empty circles) and the maximum probability curve (continuous line). The calculations were performed assuming that in the absence of errors ( $E = 0$ ) there exists a perfect enthalpy-entropy straight line with a slope equal either to the experimental isokinetic temperature (627 K, left) or to the temperature leading to a situation where the experimental point matches exactly the prediction of the maximum probability curve (681 K, right). The accidental errors allowed to the rate constants varied within the range 0–100%.

The error-tolerated limits of that temperature were found by repetition of the same procedure, this time replacing the experimental isokinetic temperature ( $627 \pm 52$  K) by its allowed limits (575 and 679 K), yielding the result of  $681 \pm 45$  K. The maximum probability curves corresponding to those temperatures are shown in Figure 10.

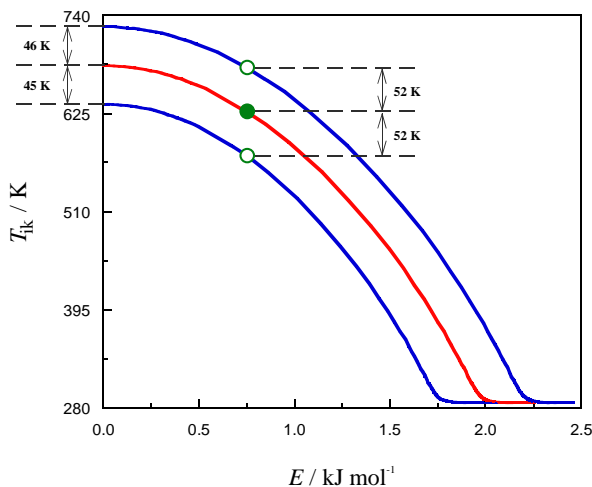


Figure 10. Isokinetic temperature as a function of the fitting error for the simulated enthalpy-entropy compensation plots based on the oxidation of a series of substituted cinnamic acids by tributylmethylammonium permanganate in methylene chloride solutions, showing the experimental point (filled circle) and its error-tolerated limits (empty circles), as well as the maximum probability curves beginning at 636, 681 and 727 K (continuous lines).

$T_{ik,exp}$ [K]	$T_{ik,sim}$ [K]	Accidental error [%]
575	636	3.39
627	681	2.94
679	727	2.59

(a)  $T_{ik,exp}$  are the experimental isokinetic temperature and its error-tolerated limits.

(b)  $T_{ik,sim}$  are the most probable simulated isokinetic temperature and its error-tolerated limits.

(c) The accidental percent error corresponds to the maximum imprecision allowed to the rate constants.

Table 1. Experimental and simulated ( $E$ -based) kinetic compensation data for the oxidation of a series of substituted cinnamic acids by tributylmethylammonium permanganate in methylene chloride solutions according to the maximum probability curve procedure.

According to the calculations, the upper bound of the random errors associated with the experimental rate constants (for this example taken from the chemical literature) was  $3.0 \pm 0.4$  % (Table 1).

The above described procedure may be repeated, now using the correlation coefficient ( $r$ ) instead of the fitting error ( $E$ ) as a measure of the quality of the linear enthalpy-entropy plot, yielding the results shown below for the maximum probability curves starting either at the coordinates ( $r = 1$ ,  $T_{ik} = 627$  K) of the point corresponding to the experimental isokinetic temperature (Figure 11, left) or to those ( $r = 1$ ,  $T_{ik} = 713$  K) of the point corresponding to the highest probability value of the isokinetic temperature (Figure 11, right).

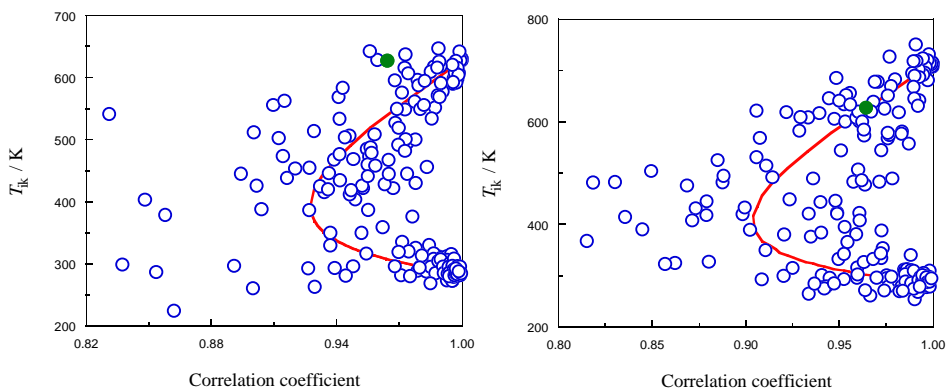


Figure 11. Isokinetic temperature as a function of the correlation coefficient for the simulated enthalpy-entropy compensation plots based on the oxidation of a series of substituted cinnamic acids by tributylmethylammonium permanganate in methylene chloride solutions, showing the experimental point (filled circle), the points obtained from computer simulations incorporating accidental errors (empty circles) and the maximum probability curve (continuous line). The calculations were performed assuming that in the absence of errors ( $r = 1$ ) there exists a perfect enthalpy-entropy straight line with a slope equal either to the experimental isokinetic temperature (627 K, left) or to the temperature leading to a situation where the experimental point matches exactly the prediction of the maximum probability curve (713 K, right).

The error-tolerated limits of that temperature were found as described above, replacing again the experimental isokinetic temperature ( $627 \pm 52$  K) by its allowed limits (575 and 679 K), yielding the result of  $714 \pm 53$  K. The maximum probability curves corresponding to those temperatures are shown in Figure 12.

This time (according to the  $r$ -based calculations) the upper bound of the random errors associated with the experimental rate constants was  $3.8 \pm 0.3 \%$  (Table 2), slightly higher than the value obtained from the  $E$ -based calculations.

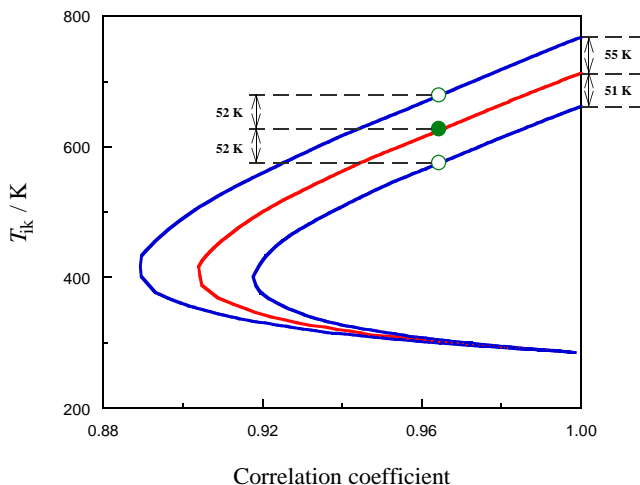


Figure 12. Isokinetic temperature as a function of the linear correlation coefficient for the simulated enthalpy-entropycompensation plots based on the oxidation of a series of substituted cinnamic acids by tributylmethylammonium permanganate in methylene chloride solutions, showing the experimental point (filled circle) and its error-tolerated limits (empty circles), as well as the maximum probability curves beginning at 662, 713 and 767 K (continuous lines).

$T_{ik,exp}$ [K]	$T_{ik,sim}$ [K]	Accidental error [%]
575	662	4.06
627	713	3.70
679	767	3.50

(a)  $T_{ik,exp}$  are the experimental isokinetic temperature and its error-tolerated limits.

(b)  $T_{ik,sim}$  are the most probable simulated isokinetic temperature and its error-tolerated limits.

(c) The accidental percent error corresponds to the maximum imprecision allowed to the rate constants.

Table 2. Experimental and simulated ( $r$ -based) kinetic compensation data for the oxidation of a series of substituted cinnamic acids by tributylmethylammonium permanganate in methylene chloride solutions according to the maximum probability curve procedure.



On the other hand, another way to find the highest probability value of the isokinetic temperature would be to focus on the number of simulations leading to points placed close enough to the experimental one, rather than on the concept of maximum probability curve. The simulations accepted as valid in this new strategy were those leading to statistical parameters within a ten percent margin of the experimental values:  $T_{ik} = 627 \pm 52$  K and either  $E = 0.75$  kJ mol<sup>-1</sup> ( $T_{ik}-E$  plane) or  $1-r = 0.036$  ( $T_{ik}-r$  plane), depending on the kind of method:

$$0.9 (T_{ik})_{exp} \leq (T_{ik})_{sim} \leq 1.1 (T_{ik})_{exp} \quad (18)$$

$$0.9 E_{exp} \leq E_{sim} \leq 1.1 E_{exp} \quad (19)$$

$$0.9 (1 - r_{exp}) \leq 1 - r_{sim} \leq 1.1 (1 - r_{exp}) \quad (20)$$

Whereas in the cases of the isokinetic temperature and the fitting error the 10% amplitude range was established with respect to the experimental values of those magnitudes, in the case of the correlation coefficient it was opted to take that range with respect to the experimental value of  $1-r$ , so as to ensure that the possibility of  $r_{sim} > 1$  was avoided.

The implementation of these conditions is illustrated in the examples shown in the following graphs, where it can be observed that a change in the slope assumed for the enthalpy-entropy compensation plot from the experimental value (Figures 13 and 14, left) to the extrapolated maximum probability values (Figures 13 and 14, right) results in an increase of the density of points placed on the regions considered as valid according to eqs 18-20.

The number of simulations performed in each case was  $10^6$ , changing from one to another the random errors associated to the rate constants at the different temperatures. This procedure was repeated taking for  $(T_{ik})_{exp}$  in eq 18 either the experimental value of the isokinetic temperature (627 K) or its error-tolerated limits (575 and 679 K). The probability curves so obtained presented maxima slightly shifted toward higher temperatures for the  $r$ -based method (Figure 15, right) with respect to the  $E$ -based method (Figure 15, left).

The resulting data are compiled in Table 3, yielding for the extrapolated most probable isokinetic temperatures the values  $677 \pm 36$  K ( $E$ -based) and  $702 \pm 60$  K ( $r$ -based).

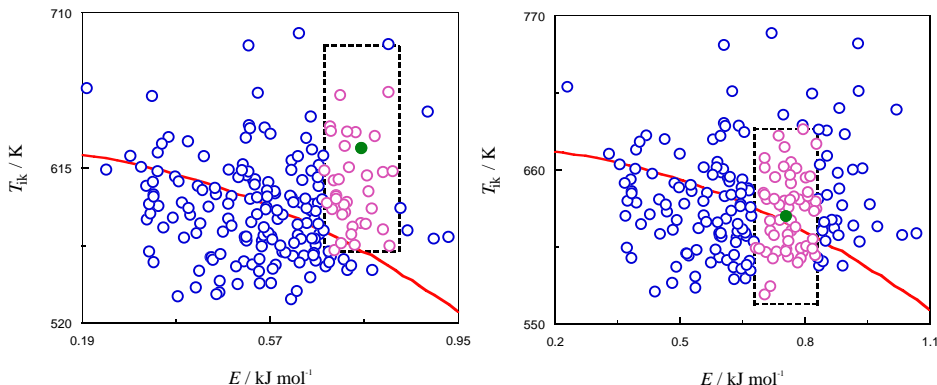


Figure 13. Isokinetic temperature as a function of the fitting error for the simulated enthalpy-entropy compensation plots based on the case under study, showing the experimental point (filled circle), the points obtained from computer simulations incorporating accidental errors (empty circles) and the maximum probability curve (continuous line). The calculations were performed assuming that in the absence of errors ( $E = 0$ ) there exists a perfect enthalpy-entropy straight line with a slope equal either to the experimental (627 K, left) or the maximum probability (677 K, right) values of the isokinetic temperature. The accidental errors allowed to the rate constants varied within the range 2.59–3.39%. The dashed lines show the limits of the regions corresponding to potentially valid simulations.

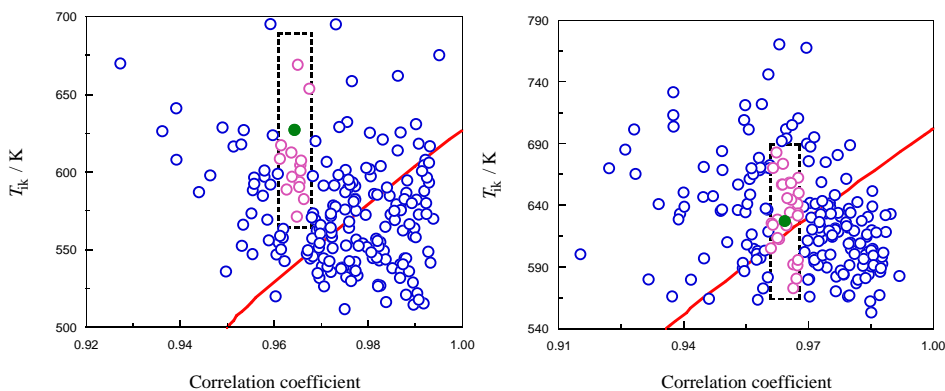


Figure 14. Isokinetic temperature as a function of the correlation coefficient for the simulated enthalpy-entropy compensation plots based on the case under study, showing the experimental point (filled circle), the points obtained from computer simulations incorporating accidental errors (empty circles) and the maximum probability curve (continuous line). The calculations were performed assuming that in the absence of errors ( $r = 1$ ) there exists a perfect enthalpy-entropy straight line with a slope equal either to the experimental (627 K, left) or the maximum probability (702 K, right) values of the isokinetic temperature. The accidental errors allowed to the rate constants varied within the range 3.50–4.06%. The dashed lines show the limits of the regions corresponding to potentially valid simulations.

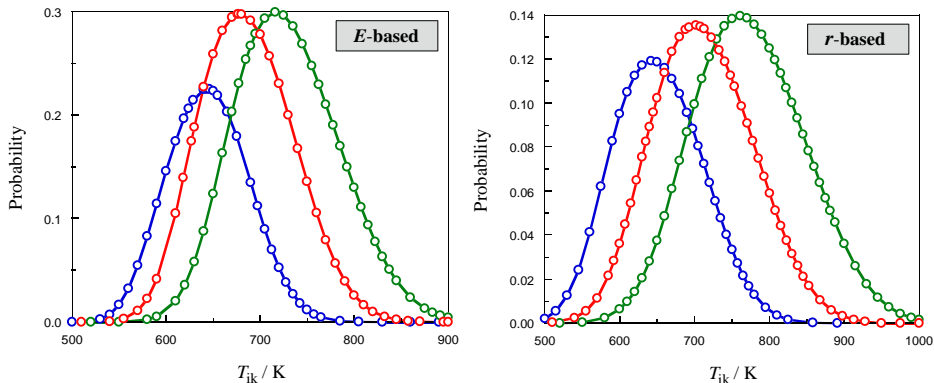


Figure 15. Probability as a function of the extrapolated (error-free) isokinetic temperature for the simulated enthalpy-entropy compensation plots based on the oxidation of a series of substituted cinnamic acids by tributylmethylammonium permanganate in methylene chloride solutions. The calculations were performed assuming that the laboratory obtained (error-prone) isokinetic temperature was equal either to the experimental value (627 K, middle curves) or to its error-tolerated inferior (575 K, highest curves) and superior (679 K, lowest curves) limits. The accidental errors allowed to the rate constants varied within the ranges either 0.00–3.39% (*E*-based method, left) or 0.00–4.06% (*r*-based method, right).

	<i>E</i> -based method		<i>r</i> -based method
$T_{ik,exp}$ [K]	$T_{ik,sim}$ [K]		$T_{ik,sim}$ [K]
575	645		642
627	677		702
679	716		761

- (a) Parameter *E* is the experimental fitting error of the enthalpy-entropy compensation plot.  
 (b) Parameter *r* is the experimental correlation coefficient of the enthalpy-entropy compensation plot.  
 (c)  $T_{ik,exp}$  are the experimental isokinetic temperature and its error-tolerated limits.  
 (d)  $T_{ik,sim}$  are the most probable simulated isokinetic temperature and its error-tolerated limits.

Table 3. Experimental and simulated (either *E*-based or *r*-based) isokinetic temperatures for the oxidation of a series of substituted cinnamic acids by tributylmethylammonium permanganate in methylene chloride solutions according to the point-counting procedure.

The values of the extrapolated isokinetic temperature, as well as their corresponding error limits, obtained from the four different methods employed so far (maximum probability curve and point counting, each in its *E*- or *r*-based version) can be compared in Table 4.

Method	<i>E</i> -based	<i>r</i> -based
Maximum probability curve	681 ± 45	713 ± 53
Point-counting	677 ± 36	702 ± 60

(a) Parameter *E* is the experimental fitting error of the enthalpy-entropy compensation plot.

(b) Parameter *r* is the experimental correlation coefficient of the enthalpy-entropy compensation plot.

Table 4. Highest probability values of the extrapolated isokinetic temperature (in K) for the oxidation of a series of substituted cinnamic acids by tributylmethylammonium permanganate in methylene chloride solutions according to the different methods.

It can be concluded that, although the extrapolated data are notably consistent, the *r*-based methods yield more divergent results (differing in 11 K) than their *E*-based counterparts (differing in 4 K), besides their imprecisions being higher (53 - 60 K vs. 36 - 45 K). Moreover, given that the *E*-methods lead to comparable results, the maximum probability curve version should be preferred over the point-counting one, not only because the former does not require any relatively arbitrary condition as the latter (the 10% amplitude range, eqs 18-20), but also because it can be implemented in a more automatized way (does not require a point by point curve building).

By way of summary, it can be concluded that, although the experimental data for the currently analyzed case yielded a linear compensation plot with a slope equal to 627 ± 52 K, the actual isokinetic temperature (once discounted the effect of random errors) was probably 681 ± 45 K, the deviation being attributable to the accidental type imprecisions made in the determination of the rate constants, since the randomness of the latter results in a bias so that the slope of the enthalpy-entropy correlation moves toward the mean experimental temperature (286 K).

## 9. APPLICATION TO BIBLIOGRAPHIC DATA

### 9.1. PHYSICAL MODEL: DOUBLING TEMPERATURE VALUES

Once arrived here, it is convenient to stop and think on the main purpose of the present work. It can be formulated as finding an answer to the following questions:

*First:* Why, within the realm of a homologous reaction series, the activation energy may change considerably from one member to another, whereas the rate constant does not vary so much?

*Second:* Does it mean that the dependence of the rate constant on temperature cannot be described by a simple exponential function?

*First question – experimental facts:* The kinetic data reported in the chemical literature for different homologous reaction series have been used to calculate the expected and found values of the rate constant ratio from the Arrhenius equation as:

$$\left( \frac{k_1}{k_2} \right)_e = e^{\frac{E_{a,2} - E_{a,1}}{RT_m}} \quad (21)$$

$$\left( \frac{k_1}{k_2} \right)_f = \frac{A_1}{A_2} e^{\frac{E_{a,2} - E_{a,1}}{RT_m}} \quad (22)$$

where  $T_m$  is the experimental mean temperature, and  $E_{a,1}$  and  $E_{a,2}$  the lowest and highest activation energies within each series, respectively.

As shown in both Figure 16 and Table 1-A (Appendix 4), the values of the rate constant ratio experimentally found in the laboratories<sup>43, 49, 58-68</sup> were consistently lower than those expected according to eq 21, in which only the information contained in the activation energies was considered. This is a reflection of the phenomenon known as kinetic compensation effect, since an increase in the activation energy usually comes with a parallel increase in the Arrhenius pre-exponential factor. In particular, when within the same reaction series the activation energies are different enough, an expected ratio of 15 orders of magnitude may be reduced to only 2 orders as seen in the actual experiments.

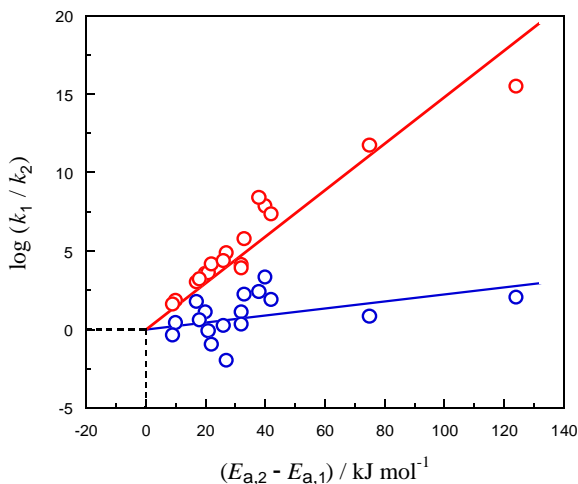


Figure 16. Expected (red points) and found (blue points) values of the logarithm of the rate constant ratio at the mean experimental temperature for two members of each homologous reaction series taken from bibliographic sources as a function of the difference between the corresponding lowest ( $E_{a,1}$ ) and highest ( $E_{a,2}$ ) activation energies. The dashed lines mark the intersection of the two straight lines at the origin of coordinates.

*Second question – modified Arrhenius equation as a potential answer:* As has been demonstrated before, if it is assumed that the activation energy increases with temperature in either an exact or approximate linear way, the pre-exponential factor also increases (eq 6). Thus, whereas according to the original version of the Arrhenius equation (eq 5) the rate constant extrapolated at  $T = \infty$  would be a finite magnitude (the pre-exponential factor):

$$\lim_{T \rightarrow \infty} k_{AE} = A \quad (23)$$

according to the modified version of the same equation the extrapolated rate constant would be an infinite magnitude:

$$\lim_{T \rightarrow \infty} k_{MAE} = \infty \quad (24)$$

This result seems indeed logical if taken into account that the pre-exponential factor is at least partially related with the frequency of reactant collisions per unit volume, parameter expected to

increase indefinitely as the temperature increases (the Arrhenius equation does not account for its temperature dependence).

First of all, an important point that should be conveniently addressed is whether eq 6 may be coherent or not with the usually Arrhenius fulfilling experimental data. Actually, if  $\ln k_{AE}$  vs.  $1/T$  is a linear relationship, it follows straightforwardly that  $\ln k_{MAE}$  vs.  $1/T$  cannot lead to a perfect linear plot. However, as shown in Figure 17 (left), provided that the exponent of the temperature in the pre-exponential factor is low enough, the Arrhenius plot would be acceptably linear for a temperature range as wide as 900 K (much more than reported in most kinetic studies).

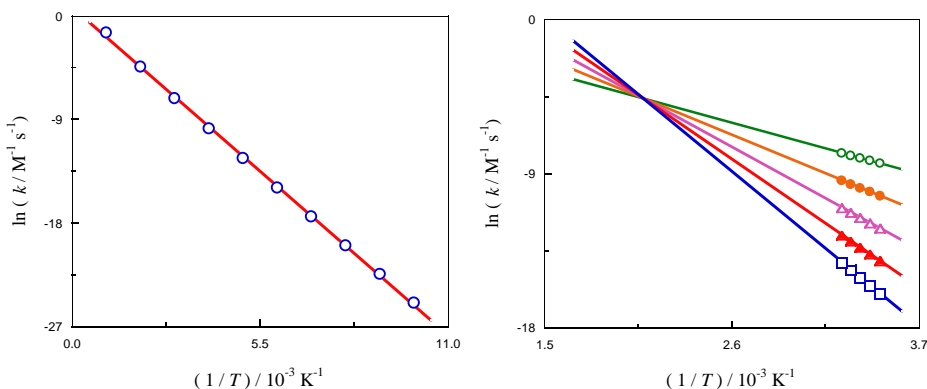


Figure 17. Arrhenius plots for the simulation of reactions fulfilling the modified Arrhenius equation with  $A_E = 1.00 \times 10^{-2} \text{ M}^{-1} \text{ s}^{-1}$  and  $T_d = 3000 \text{ K}$ . Left: a single reaction with  $E_{a,o} = 20 \text{ kJ mol}^{-1}$  at  $T = 100 - 1000 \text{ K}$  ( $r = 0.99974$ ). Right: a five reaction homologous series with  $E_{a,o} = 20$  (empty circles), 30 (filled circles), 40 (empty triangles), 50 (filled triangles) and 60 (squares)  $\text{kJ mol}^{-1}$  at  $T = 15.0 - 35.0 \text{ }^\circ\text{C}$  ( $T_m = 298 \text{ K}$ ), showing an isokinetic temperature at  $492 \text{ K}$ .

Moreover, the modified Arrhenius equation leads to perfectly behaved isokinetic plots (Figure 17, right) with the only requirement that the doubling temperature ( $T_d$ ) remains constant along the reaction series. According to eqs 13 and 16, the isokinetic and doubling temperatures would then be:

$$T_{ik} = \frac{T_m + T_d}{1 + \ln T_m} \quad (25)$$

$$T_d = (1 + \ln T_m) T_{ik} - T_m \quad (26)$$

The values of parameter  $T_d$  calculated from eq 26 for different homologous reaction series reported in the literature appear compiled in Table 2-A (Appendix 4).

## 9.2. SEEKING THE TRUE ISOKINETIC TEMPERATURE: HIGHEST PROBABILITY VALUES

The Arrhenius equation allows writing the ratio of rate constants determined at the same absolute temperature ( $T$ ) as:

$$\left( \frac{k_1}{k_2} \right)_T = \frac{A_1}{A_2} e^{\frac{E_{a,2} - E_{a,1}}{RT}} \quad (27)$$

where the subscripts 1 and 2 correspond to the reactions with the lowest and highest activation energies of the homologous series, respectively. Given that in the particular case of  $T = T_{ik}$  the rate constants for the different family members are known to take identical values, it can be concluded that:

$$\left( \frac{k_1}{k_2} \right)_{T_{ik}} = \frac{A_1}{A_2} e^{\frac{E_{a,2} - E_{a,1}}{RT_{ik}}} = 1 \quad (28)$$

and consequently:

$$\frac{A_1}{A_2} = e^{\frac{E_{a,1} - E_{a,2}}{RT_{ik}}} \quad (29)$$

Finally, from eq 27 (at  $T = T_m$ ) and eq 29 it follows that:

$$\left( \frac{k_1}{k_2} \right)_{T_m} = e^{\frac{E_{a,2} - E_{a,1}}{R} \left( \frac{1}{T_m} - \frac{1}{T_{ik}} \right)} \quad (30)$$

Therefore, three different alternatives are possible depending on the value of the mean experimental temperature (Scheme 1). As can be seen in Table 1-A (Appendix 4), from the 17 homologous reaction series consulted in the literature, the predominant situation was that of ratio  $> 1$  (76%), whereas that of ratio  $< 1$  accounted only for a small fraction (24%). Since the first particular case has already been addressed in depth in a previous section, now the attention will be focused on the second.



$$T_m < T_{ik} \Rightarrow \left( \frac{k_1}{k_2} \right)_{T_m} > 1$$

$$T_m = T_{ik} \Rightarrow \left( \frac{k_1}{k_2} \right)_{T_m} = 1$$

$$T_m > T_{ik} \Rightarrow \left( \frac{k_1}{k_2} \right)_{T_m} < 1$$

Scheme 1. Values of the rate constant ratio under different experimental conditions of the mean working temperature in relation to the isokinetic temperature of the homologous reaction series.

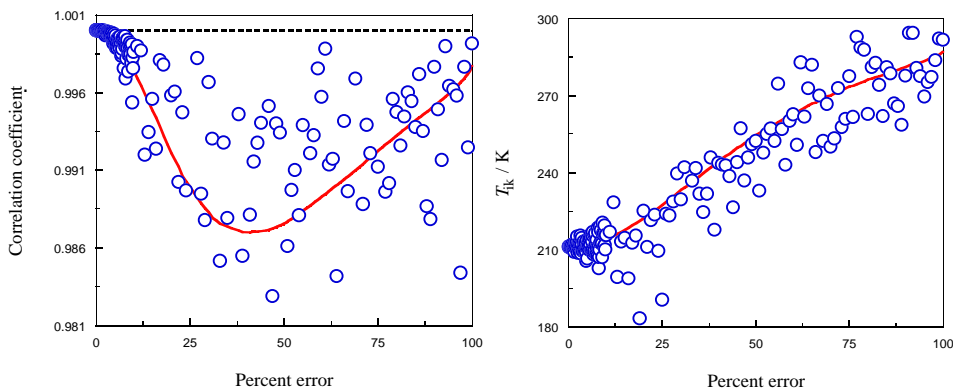


Figure 18. Correlation coefficient (left) and isokinetic temperature (right) as functions of the maximum limit allowed to the percent random errors of the rate constants for the simulated compensation plots based on the oxidation of blue copper proteins by tris(1,10-phenanthroline)cobalt(III) ion, assuming that in the absence of errors there exists a perfect enthalpy-entropy straight line with a slope equal to the experimental isokinetic temperature (211 K). The dashed line corresponds to a perfect enthalpy-entropy correlation ( $r = 1$ ) and the continuous lines to the maximum probability curves.

It might be interesting to know the aspect of the simulation graphs in those particular cases where the mean experimental temperature is higher than the isokinetic temperature ( $T_m > T_{ik}$ ).

To that end, the series chosen as an example was that of the oxidation of blue copper proteins by tris(1,10-phenanthroline)cobalt(III) ion.<sup>63</sup> Again, it was observed that, as the experimental accidental errors of the rate constants increased, the correlation coefficient of the compensation plot first decreased, passed through a minimum and then increased (Figure 18, left). However, the slope increased this time from the experimental isokinetic temperature to values close to the mean working temperature (Figure 18, right).

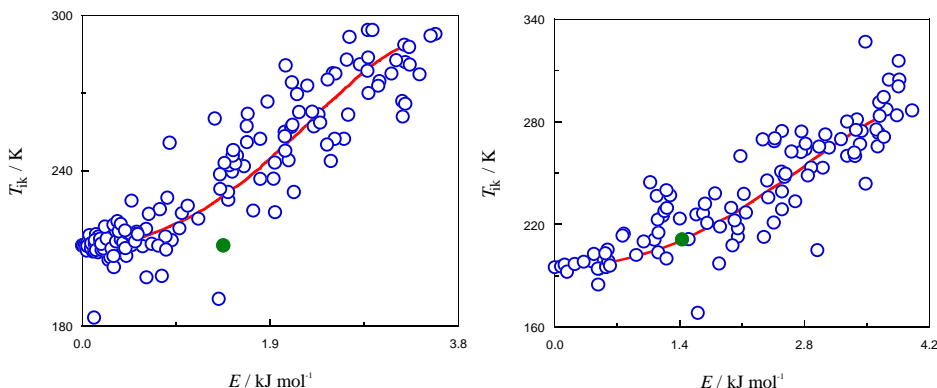


Figure 19. Isokinetic temperature as a function of the fitting error for the simulated enthalpy-entropy compensation plots based on the oxidation of blue copper proteins by tris(1,10-phenanthroline)cobalt(III) ion, showing the experimental point (filled circle), the points obtained from computer simulations incorporating accidental errors (empty circles) and the maximum probability curve (continuous line). The calculations were performed assuming that in the absence of errors ( $E = 0$ ) there exists a perfect enthalpy-entropy straight line with a slope equal either to the experimental isokinetic temperature (211 K, left) or to the temperature leading to a situation where the experimental point matches exactly the prediction of the maximum probability curve (195 K, right). The accidental errors allowed to the rate constants varied within the range 0–100%.

Accordingly, the simulated isokinetic temperature increased from either the experimental value (Figure 19, left) or the extrapolated maximum probability value (Figure 19, right) to the mean working temperature as the fitting activation enthalpy error increased.

Once more, the procedure was repeated, now assessing the quality of the linear compensation plot by means of the correlation coefficient ( $r$ ) instead of the fitting error ( $E$ ), yielding the results represented below for the maximum probability curves starting either at the coordinates ( $r = 1$ ,  $T_{ik} = 211$  K) of the point corresponding to the experimental isokinetic temperature (Figure 20, left) or to those ( $r = 1$ ,  $T_{ik} = 196$  K) of the point corresponding to the extrapolated highest probability value of the isokinetic temperature (Figure 20, right).

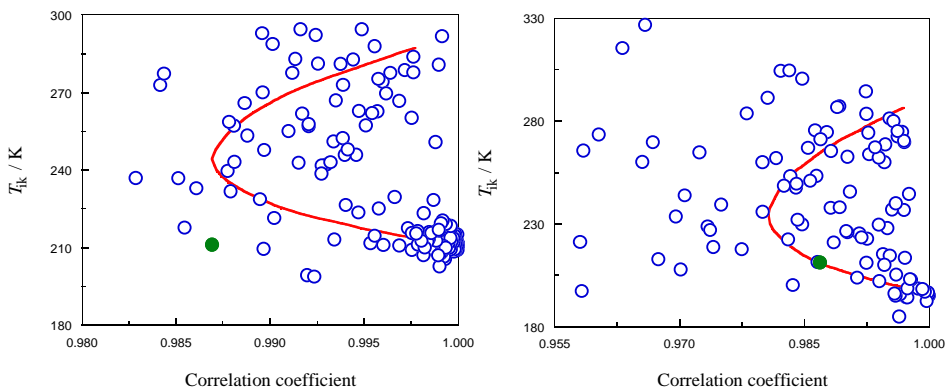


Figure 20. Isokinetic temperature as a function of the correlation coefficient for the simulated enthalpy-entropy compensation plots based on the oxidation of blue copper proteins by tris(1,10-phenanthroline)cobalt(III) ion, showing the experimental point (filled circle), the points obtained from computer simulations incorporating accidental errors (empty circles) and the maximum probability curve (continuous line). The calculations were performed assuming that in the absence of errors ( $r = 1$ ) there exists a perfect enthalpy-entropy straight line with a slope equal either to the experimental isokinetic temperature (211 K, left) or to the temperature leading to a situation where the experimental point matches exactly the prediction of the maximum probability curve (196 K, right). The accidental errors allowed to the rate constants varied within the range 0 – 100%.

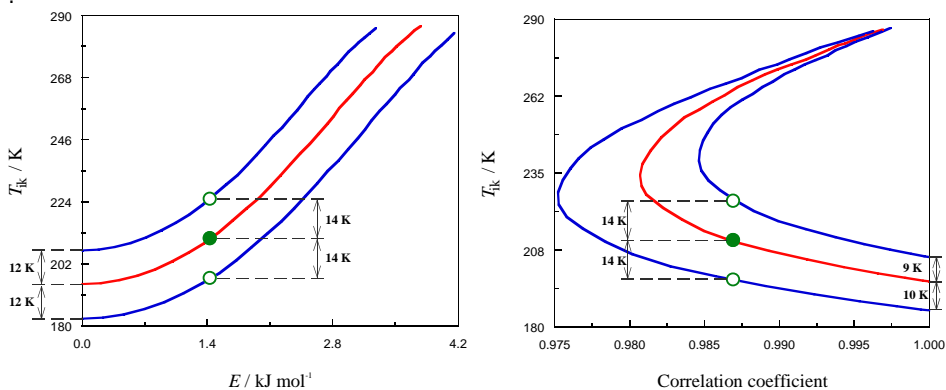


Figure 21. Isokinetic temperature as a function of either the fitting error (left) or the correlation coefficient (right) for the simulated enthalpy-entropy compensation plots based on the oxidation of blue copper proteins by tris(1,10-phenanthroline)cobalt(III) ion, showing the experimental point (filled circle) and its error-tolerated limits (empty circles), as well as the maximum probability curves (continuous lines) beginning either at 183, 195 and 207 K ( $E$ -based method) or at 186, 196 and 205 K ( $r$ -based method).

The error-tolerated limits of the extrapolated isokinetic temperature were found by repetition of the numerical simulation procedure, this time replacing the experimental value ( $211 \pm 14$  K)

by its allowed limits (197 and 225 K), yielding the results of  $195 \pm 12$  K ( $E$ -based method, Figure 21, left) and  $196 \pm 10$  K ( $r$ -based method, Figure 21, right).

The values of the extrapolated isokinetic temperature obtained by the  $E$ -based version of the maximum probability curve method for different homologous reaction series selected from the specialized literature appear compiled in Table 2-A (Appendix 4). A mere inspection of them reveals that (as shown in Figure 22, left), when the experimental isokinetic temperature is higher than the mean working temperature ( $T_{ik,exp} > T_m$ ), the extrapolated value should be looked for in the high temperature range ( $T_{ik,sim} > T_{ik,exp}$ ). On the contrary, when the experimental isokinetic temperature is lower than the mean working temperature ( $T_{ik,exp} < T_m$ ), the extrapolated value should be looked for in the low temperature range ( $T_{ik,sim} < T_{ik,exp}$ ). This is so because the random errors provoke a shift of the experimental isokinetic temperature toward the mean working temperature ( $T_{ik,exp} \rightarrow T_m$ ).

Further, the relative error of the extrapolated isokinetic temperature decreased dramatically as the correlation coefficient of the enthalpy-entropy linear plot increased (Figure 22, right). On the other hand, it should be noticed that the higher values of parameter  $E$  ( $k$ ) might not be entirely attributable to experimental errors of the rate constants, but rather to the own nature of each chemical reaction: according to the physical model proposed in the present work, parameter  $T_d$  might be slightly different for each member of the homologous series.

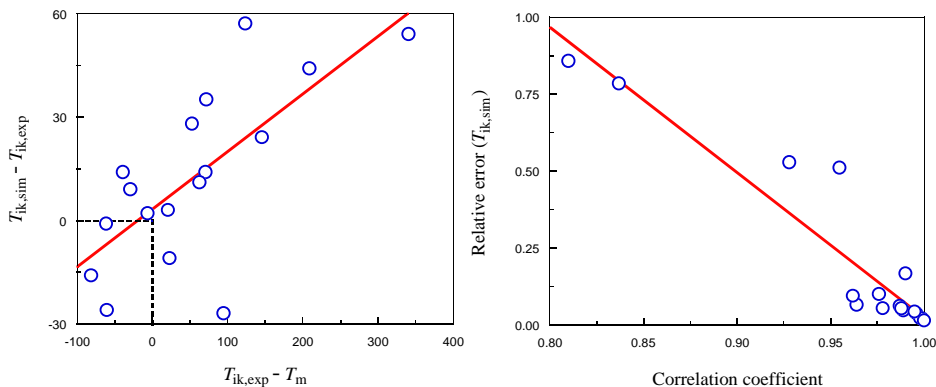


Figure 22.  $T_{ik,sim} - T_{ik,exp}$  as a function of  $T_{ik,exp} - T_m$  (left) and the relative error of  $T_{ik,sim}$  as a function of the correlation coefficient of the isokinetic plot (right) for different homologous reaction series taken from the chemical literature. The dashed lines mark out the area corresponding to the points with double negative coordinates ( $T_{ik,exp} < T_m \Rightarrow T_{ik,sim} < T_{ik,exp}$ ).

## 10. CONCLUSIONS

(i) The compensation effect is a widespread phenomenon, spanning over the fields of both physics and chemistry. This seems to call for a general explanation, the main potential alternatives being: the ubiquitous experimental errors (either accidental or systematic) and the effect of temperature on the activation energy.

(ii) A certain dependence of the Arrhenius parameters on temperature cannot be discarded, since the frequency of reactant collisions per unit volume and the occupation number of each electronic energy level (for the reactants and the activated complex) are both strongly temperature-dependent.

(iii) The Arrhenius parameters are interconnected, so that an increase (or decrease) of the activation energy with temperature results in an increase (or decrease) of the pre-exponential factor (and vice versa).

(iv) The modified Arrhenius and Eyring equations (physical model) can explain the kinetic compensation effect unless the doubling temperature is directly proportional to the activation energy at 0 K (situation that seems implausible for physico-chemical reasons).

(v) According to the bibliographic kinetic data, the values obtained for the doubling temperature (in the range 819 – 3887 K) are high enough to be consistent with almost linear  $\ln k$  vs.  $1/T$  plots (linearized Arrhenius equation).

(vi) That physical model seems to be supported by the low values of parameter  $T_d$  obtained for chemical reactions involving either proteins or biomimetic enzyme-like complexes as reactants (819 – 1416 K) when compared with the remaining data (1557– 3887 K).

(vii) The random errors provoke a shift of the experimental isokinetic temperature toward the mean working temperature. By discounting this effect, the most probable (extrapolated) value of the isokinetic temperature can be found.

(viii) When the experimental isokinetic temperature is higher (lower) than the mean working temperature, the extrapolated value should be looked for in the high (low) temperature range:  $T_{ik,sim} > T_{ik,exp}$  (or  $T_{ik,sim} < T_{ik,exp}$ ).

(ix) The high values of parameter  $E(k)$  found for some homologous series might indicate that, due to the own nature of each chemical reaction, the doubling temperature might be slightly different for each member of the series.

## 11. REFERENCES

1. Constable, F. H. The Mechanism of Catalytic Decomposition. *Proc. R. Soc. London A* **1925**, *108*, 355-378.
2. Leffler, J. E. The Enthalpy-Entropy Relationship and its Implications for Organic Chemistry. *J. Org. Chem.* **1955**, *20*, 1202-1231.
3. Linert, W.; Jameson, R. F. The Isokinetic Relationship. *Chem. Soc. Rev.* **1989**, *18*, 477-505.
4. Linert, W. Mechanistic and Structural Investigations Based on the Isokinetic Relationship. *Chem. Soc. Rev.* **1994**, *23*, 429-438.
5. Liu, L.; Guo, Q. X. Isokinetic Relationship, Isoequilibrium Relationship, and Enthalpy-Entropy Compensation. *Chem. Rev.* **2001**, *101*, 673-695.
6. Lyon, R. E. Isokinetics. *J. Phys. Chem.* **2019**, *123*, 2462-2469.
7. Pinheiro, L. M. V.; Calado, A. R. T.; Reis J. C. R. The Quaternisation Reaction of Phosphines and Amines in Aliphatic Alcohols. A Similarity Analysis Using the Isokinetic, Isosolvent and Isoselective Relationships. *Org. Biomol. Chem.* **2004**, *2*, 1330-1338.
8. Govardan, D.; Bhooshan, M.; Saiprakash, P. K.; Rajanna, K. C. Trichloroisocyanuric Acid and NaNO<sub>2</sub> Mediated Nitration of Indoles under Acid-Free and Vilsmeier-Haack Conditions: Synthesis and Kinetic Study. *SN Appl. Sci.* **2019**, *1*, 1004.
9. Linert, W. The Isokinetic Relationship. 6. Equilibrium Systems. *Chem. Phys.* **1987**, *114*, 457-462.
10. Sugihara, G.; Shigematsu, D. S.; Nagadome, S. Thermodynamic Study on the Langmuir Adsorption of Various Bile Salts Including Taurine and Glycine Conjugates onto Graphite in Water. *Langmuir* **2000**, *16*, 1825-1833.
11. Davidovits, P.; Jayne, J. T.; Duan, S. X.; Wornsop, D. R.; Zahinser, M. S.; Kolb, C. E. Uptake of Gas Molecules by Liquids – A Model. *J. Phys. Chem.* **1991**, *95*, 6337-6340.
12. Nathanson, G. M.; Davidovits, P.; Wornsop, D. R.; Kolb, C. E. Dynamics and Kinetics at the Gas-Liquid Interface. *J. Phys. Chem.* **1996**, *100*, 13007-13020.
13. Waring, C. E.; Becher, P. Structure in Liquids and the Relation Between the Parameters of the Arrhenius Equation for Reactions in the Condensed Phase. *J. Chem. Phys.* **1947**, *15*, 488-496.
14. Shimakawa, K.; Aniya, M. Dynamics of Atomic Diffusion in Condensed Matter: Origin of the Meyer-Neldel Compensation Law. *Monatsh. Chem.* **2013**, *144*, 67-71.
15. Sagotra, A. K.; Chu, D.; Cazorla, C. Influence of Lattice Dynamics on Lithium Ion Conductivity: A First Principles Study. *Phys. Rev. Mater.* **2019**, *3*, 035405.
16. Sedivy, L.; Belas, E.; Grill, R.; Musiienko, A.; Vasylychenko, I. Extension of Meyer-Neldel Rule Using Chemical Diffusion Experiments in CdTe. *J. Alloys. Compd.* **2019**, *788*, 897-904.
17. Crine, J. P. The Compensation Law in Dielectric Polymer Relaxations. *Monatsh. Chem.* **2013**, *144*, 11-19.
18. Crandall, R. S. Defect Relaxation in Amorphous Silicon: Stretched Exponentials, the Meyer-Neldel Rule, and the Staebler-Wronski Effect. *Phys. Rev. B* **1991**, *43*, 4057-4070.
19. Srivastava, A.; Sharma, S. D.; Metha, N. Signature of Meyer-Neldel Compensation Rule in Iso-Conventional Crystallisation under the Influence of  $\gamma$ -Ray Irradiation. *Ceram. Int.* **2018**, *44*, 20827-20834.
20. Engstrom, O. Compensation Effects at Electron Traps in Semiconductors. *Monatsh. Chem.* **2013**, *144*, 73-82.
21. Rosenberg, B.; Bhowmik, B. B.; Harder, H. C.; Postow, E. Pre-Exponential Factor in Semiconducting Organic Substances. *J. Chem. Phys.* **1968**, *49*, 4108-4114.
22. Ashraf, I. M.; El-Zahhar, A. A. Studies on the Photoelectric Properties of Crosslinked-Poly(Acrylamide Co-Acrylic Acid) for Photo Detector Applications. *Results. Phys.* **2018**, *11*, 842-846.
23. He, Q.; Xu, X.; Gu, Y.; Cheng, X.; Xu, J.; Jiang, Y. Single-Walled Carbon Nanotube-Controlled Meyer-Neldel Rules in Vanadium Oxide Films for Applications as Thermistor Materials in Sensors and Detectors. *ACS Appl. Nano Mater.* **2018**, *1*, 6959-6966.

24. Kumar, A.; Mehta, N. Universality of Meyer-Neldel Compensation Rule (MNCR): Case Study of Thermally Assisted A.C. Conduction after Laser Irradiation. *J. Phys. Chem. Solids*. **2018**, *121*, 49-53.
25. Biswas, D.; Singh, L. S.; Das, A. S.; Bhattacharya, S. An Investigation of Te-Se Semiconducting Glassy Alloys: Structural Characterization and Electrical Conductivity. *J. Non-Cryst. Solids*. **2019**, *510*, 101-111.
26. Freed, K. F. Entropy-Enthalpy Compensation in Chemical Reactions and Adsorption: An Exactly Solvable Model. *J. Phys. Chem. B* **2011**, *115*, 1689-1692.
27. Moyano, P. C.; Zuñiga, R. N. Enthalpy-Entropy Compensation for Browning of Potato Strips during Deep-Fat Frying. *J. Food. Eng.* **2004**, *63*, 57-62.
28. Barrie, P. J. The Mathematical Origins of the Kinetic Compensation Effect: 1. The Effect of Random Experimental Errors. *Phys. Chem. Chem. Phys.* **2012**, *14*, 318-326.
29. Perez-Benito, J. F. Some Tentative Explanations for the Enthalpy-Entropy Compensation Effect in Chemical Kinetics: From Experimental Errors to the Hinshelwood-Like Model. *Monatsh. Chem.* **2013**, *144*, 49-58.
30. Perez-Benito, J. F.; Mulero-Raichs, M. Enthalpy-Entropy Compensation Effect in Chemical Kinetics and Experimental Errors: A Numerical Simulation Approach. *J. Phys. Chem. A* **2016**, *120*, 7598-7609.
31. Koudriavtsev, A. B.; Linert, W. Do Experimental Errors Really Cause Isoequilibrium and Isokinetic Relationships? *Match-Commun. Math. Co.* **2013**, *70*, 7-28.
32. Barrie, P. J. The Mathematical Origins of the Kinetic Compensation Effect: 2. The Effect of Systematic Errors. *Phys. Chem. Chem. Phys.* **2012**, *14*, 327-336.
33. Barlow, R. *Statistics: A Guide to the Use of Statistical Methods in the Physical Sciences*; Wiley: New York, 1989.
34. Menzinger, M.; Wolfgang, R. The Meaning and Use of the Arrhenius Activation Energy. *Angew. Chem. Int. Ed.* **1969**, *8*, 438-444.
35. Jortner, J. Temperature Dependent Activation Energy for Electron Transfer between Biological Molecules. *J. Chem. Phys.* **1976**, *64*, 4860-4867.
36. Gardiner, W. C. Temperature Dependence of Bimolecular Gas Reaction Rates. *Acc. Chem. Res.* **1977**, *10*, 326-331.
37. Li, J. V.; Johnston, S. W.; Yan, Y.; Levi, D. H. Measuring Temperature-Dependent Activation Energy in Thermally Activated Processes: A 2D Arrhenius Plot Method. *Rev. Sci. Instrum.* **2010**, *81*, 033910.
38. Clark, T. C.; Dove, J. E. Examination of Possible Non-Arrhenius Behavior in the Reactions. *Can. J. Chem.* **1973**, *51*, 2147-2154.
39. Laidler, K. J. *Chemical Kinetics*; Harper Collins: New York, 1987.
40. McGillen, M. R.; Baasandorj, M.; Burkholder, J. B. Gas-Phase Rate Coefficients for the OH + *n*-, *i*-, *s*-, and *t*-Butanol Reactions Measured between 220 and 380 K: Non-Arrhenius Behavior and Site-Specific Reactivity. *J. Phys. Chem. A* **2013**, *117*, 4636-4656.
41. Nakamura, K.; Takayanagi, T.; Sato, S. A Modified Arrhenius Equation. *Chem. Phys. Lett.* **1989**, *160*, 295-298.
42. Robinson, P. J. Dimensions and Standard States in the Activated Complex Theory of Reaction Rates. *J. Chem. Educ.* **1978**, *55*, 509-510.
43. Bernhardt, P. V.; Gonzalez, M. A.; Martinez, M. Kinetic-Mechanistic Study on the Oxidation of Biologically Active Iron(II) Bis(thiosemicarbazone) Complexes by Air. Importance of NH $\cdots$ O $_2$  Interactions As Established by Activation Volumes. *Inorg. Chem.* **2017**, *56*, 14284-14290.
44. Freeman, F. Postulated Intermediates and Activated Complexes in the Permanganate Ion Oxidation of Organic Compounds. *Rev. React. Species Chem. React.* **1976**, *1*, 179-226.
45. Fatiadi, A. J. The Classical Permanganate Ion – Still a Novel Oxidant in Organic Chemistry. *Synthesis* **1987**, 85-127.
46. Singh, N.; Lee, D. G. A Green and Versatile Industrial Oxidant. *Org. Process Res. Dev.* **2001**, *5*, 599-603.

47. Perez-Benito, J. F.; Ferrando, J. Three Rate-Constant Kinetic Model for Permanganate Reactions Autocatalyzed by Colloidal Manganese Dioxide: The Oxidation of L-Phenylalanine. *J. Phys. Chem. B* **2014**, *118*, 14949-14960.
48. Lee, D. G. Phase Transfer Assisted Permanganate Oxidations. In *Oxidation in Organic Chemistry*, Part D; Trahanovsky, W. S., Ed.; Academic Press: New York, 1982.
49. Perez-Benito, J. F. Substituent Effects on the Oxidation of Cinnamic Acid by Methyltributylammonium Permanganate in Methylene Chloride. *Chem. Scr.* **1987**, *27*, 433-436.
50. Perez-Benito, J. F.; Lee, D. G. Kinetics and Mechanism of the Oxidation of Unsaturated Carboxylic Acids by Methyltributylammonium Permanganate in Methylene Chloride Solutions. *J. Org. Chem.* **1987**, *52*, 3239-3243.
51. Krug, R. R.; Hunter, W. G.; Grieger R. A. Statistical Interpretation of Enthalpy-Entropy Compensation. *Nature* **1976**, *261*, 566-567.
52. Krug, R. R.; Hunter, W. G.; Grieger R. A. Enthalpy-Entropy Compensation. 1. Some Fundamental Statistical Problems Associated with the Analysis of van't Hoff and Arrhenius Data. *J. Phys. Chem.* **1976**, *80*, 2335-2341.
53. Krug, R. R.; Hunter, W. G.; Grieger R. A. Enthalpy-Entropy Compensation. 2. Separation of the Chemical from the Statistical Effect. *J. Phys. Chem.* **1976**, *80*, 2341-2351.
54. McBane, G. C. Chemistry from Telephone Numbers: The False Isokinetic Relationship. *J. Chem. Educ.* **1998**, *75*, 919-922.
55. Sharp, K. Enthalpy-Entropy Compensation: Fact or Artifact? *Prot. Sci.* **2001**, *10*, 661-667.
56. Cornish-Bowden, A. Enthalpy-Entropy Compensation: A Phantom Phenomenon. *J. Biosci.* **2002**, *27*, 121-126.
57. Starikov, E. B.; Norden, B. Enthalpy-Entropy Compensation: A Phantom or Something Useful? *J. Phys. Chem. B* **2007**, *111*, 14431-14435.
58. Reid, L. S.; Mauk, A. G. Kinetic Analysis of Cytochrome *b<sub>5</sub>* Reduction by [Fe(EDTA)]<sup>2-</sup>. *J. Am. Chem. Soc.* **1982**, *104*, 841-845.
59. Shi, T.; Elding, L. I. Linear Free Energy Relationships for Complex Formation Reactions between Carboxylic Acids and Palladium(II). Equilibrium and High-Pressure Kinetics Study. *Inorg. Chem.* **1997**, *36*, 528-536.
60. Wiberg, K. B.; Geer, R. D. The Kinetics of the Permanganate Oxidation of Alkenes. *J. Am. Chem. Soc.* **1966**, *88*, 5827-5832.
61. Jensen, M. P.; Payeras, A. M.; Fiedler, A. T. Kinetic Analysis of the Conversion of Nonheme (Alkylperoxo)iron(III) Species to Iron(IV) Complexes. *Inorg. Chem.* **2007**, *46*, 2398-2408.
62. Liu, X.; Chen, T.; Jain, P. K.; Xu, W. Revealing the Thermodynamic Properties of Elementary Chemical Reactions at the Single-Molecule Level. *J. Phys. Chem. B* **2019**, *123*, 6253-6259.
63. McArdle, J. V.; Coyle, C. L.; Gray, H. B.; Yoneda, G. S.; Holwerda, R. A. Kinetic Studies of the Oxidation of Blue Copper Proteins by Tris(1,10-phenantroline)cobalt(III) Ions. *J. Am. Chem. Soc.* **1977**, *99*, 2483-2489.
64. Cafferata, L. F. R.; Eyley, G. N.; Svartman, E. L.; Cañizo, A. I.; Alvarez, E. Solvent Effects in the Thermal Decomposition Reactions of Cyclic Ketone Diperoxides. *J. Org. Chem.* **1991**, *56*, 411-414.
65. Wang, W. D.; Bakac, A.; Espenson, J. H. Kinetics and Mechanisms of the Redox Reactions of the Hydroperoxochromium(III) Ion. *Inorg. Chem.* **1993**, *32*, 5034-5039.
66. Kryatov, S. V.; Chavez, F. A.; Reynolds, A. M.; Rybak-Akimova, E. V.; Que, L.; Tolman, W. B. Mechanistic Studies on the Formation and Reactivity of Dioxygen Adducts of Diiron Complexes Supported by Sterically Hindered Carboxylates. *Inorg. Chem.* **2004**, *43*, 2141-2150.
67. Bedell, S. A.; Nakon, R. Isokinetic Temperatures and Mechanisms of Metal Ion Promoted Hydrolyses of Amino Acid Esters. *Inorg. Chem.* **1977**, *16*, 3055-3059.
68. Loalza, A.; Armstrong, K. M.; Baker, B. M.; Abu-Omar, M. M. Kinetics of Thermal Unfolding of Phenylalanine Hydroxylase Variants Containing Different Metal Cofactors (Fe<sup>II</sup>, Co<sup>II</sup> and Zn<sup>II</sup>) and Their Isokinetic Relationship. *Inorg. Chem.* **2008**, *47*, 4877-4883.



# APPENDICES



## APPENDIX 1: Statistical methods

The kinetic data involved in the linear correlations needed in this study were fitted by means of the least-square method, according to the following mathematical expressions:

$$a = \frac{\sum_{i=1}^N x_i^2 \sum_{i=1}^N y_i - \sum_{i=1}^N x_i \sum_{i=1}^N x_i y_i}{N \sum_{i=1}^N x_i^2 - (\sum_{i=1}^N x_i)^2} \quad b = \frac{N \sum_{i=1}^N x_i y_i - \sum_{i=1}^N x_i \sum_{i=1}^N y_i}{N \sum_{i=1}^N x_i^2 - (\sum_{i=1}^N x_i)^2} \quad (1-A)$$

$$r = \frac{N \sum_{i=1}^N x_i y_i - \sum_{i=1}^N x_i \sum_{i=1}^N y_i}{\sqrt{[N \sum_{i=1}^N x_i^2 - (\sum_{i=1}^N x_i)^2][N \sum_{i=1}^N y_i^2 - (\sum_{i=1}^N y_i)^2]}} \quad (2-A)$$

$$S_1 = \sum_{i=1}^N x_i^2 - \frac{(\sum_{i=1}^N x_i)^2}{N} \quad (3-A)$$

$$S_2 = \sqrt{\frac{1}{N-2} \left[ \sum_{i=1}^N y_i^2 - \frac{(\sum_{i=1}^N y_i)^2}{N} - b \sum_{i=1}^N x_i y_i + \frac{b^2 \sum_{i=1}^N x_i \sum_{i=1}^N y_i}{N} \right]} \quad (4-A)$$

$$E(a) = S_2 \sqrt{\frac{1}{N S_1} (\sum_{i=1}^N x_i^2)} \quad E(b) = \frac{S_2}{\sqrt{S_1}} \quad (5-A)$$

where  $x_i$  is the abscissa and  $y_i$  the ordinate of each couple of data,  $N$  the total number of points,  $a$  the intercept,  $b$  the slope,  $r$  the correlation coefficient, while  $E(a)$  and  $E(b)$  stand for the intercept and slope errors, respectively.

## APPENDIX 2: *Theoretical background: general model*

For whatever physical or chemical phenomenon involving atoms or molecules that have to overcome an activation barrier, it follows from eq 1 that:

$$\frac{d(\ln Y_T)}{dT} = \frac{X}{RT^2} \quad (6-A)$$

Now, let us assume that parameter  $X$  in eq 6-A, the energy barrier to be overcome in the activated process under consideration, depends on temperature. For the sake of simplicity, a linear dependence will be hypothesized:

$$X_T = X_o \left(1 + \frac{T}{T_d}\right) \quad (7-A)$$

where  $X_o$  is the energy barrier at  $T = 0$  K, and  $T_d$  stands for the doubling temperature, that is, the value of  $T$  at which  $X_T = 2X_o$ .

From eqs 6-A and 7-A and posterior integration:

$$\frac{d(\ln Y_T)}{dT} = \frac{X_o}{RT} \left(\frac{1}{T_d} + \frac{1}{T}\right) \quad (8-A)$$

$$\int d(\ln Y_T) = \int \frac{X_o}{RT} \left(\frac{1}{T_d} + \frac{1}{T}\right) dT \quad (9-A)$$

$$\ln Y_T = \frac{X_o}{RT_d} \ln T - \frac{X_o}{RT} + \ln A_x \quad (10-A)$$

where  $\ln A_x$  is the integration constant. Equation 10-A can also be written in its equivalent form:

$$Y_T = A_x T^{\frac{X_o}{RT_d}} e^{-\frac{X_o}{RT}} \quad (11-A)$$

where parameter  $A_x$  comes from the integration constant, its physical significance being that of the value (independent of temperature) the magnitude  $Y_T$  would take for a hypothetical non-activated process with  $X_o = 0$ .

Hence, let us assume that the correct dependence of the property  $Y_T$  on temperature is given by eq 11-A. In that case, if the experimental data are fitted according to the simplified form shown in eq 1, the fitting parameters will be (from eqs 7-A and 11-A):

$$X = X_o \left(1 + \frac{T_m}{T_d}\right) \quad (12-A)$$

$$Y_\infty = A_X (e^{T_m})^{\frac{X_o}{RT_d}} \quad (13-A)$$

where  $T_m$  is the mean value of the experimental temperature range used in the study (supposed to be short enough). Finally, from eqs 12-A and 13-A, for a series of closely related processes it could be written:

$$X_i = R \frac{T_m + T_d}{1 + \ln T_m} \ln \frac{Y_{\infty,i}}{A_X} \quad (14-A)$$

thus explaining the correlation shown in eq 2 with:

$$X_h = -R \frac{T_m + T_d}{1 + \ln T_m} \ln A_X \quad (15-A)$$

$$T_{iso} = \frac{T_m + T_d}{1 + \ln T_m} \quad (16-A)$$

provided that parameters  $T_m$ ,  $T_d$  and  $A_X$  are the same (or at least very similar) for all the members of the series. The constancy of  $T_m$  along the series is a condition easily fulfilled, because the same experimental temperature range is often used for all the processes under study.

In the case of parameter  $T_d$ , it may be justified (at least partially) by the argument that follows. According to eq 7-A, the dependence of the activation barrier on temperature is given by the derivative:

$$\frac{dX_T}{dT} = \frac{X_o}{T_d} \quad (17-A)$$

If there is a systematic change of this derivative along the series, the simplest way to take it into consideration is to assume a linear dependence on the value of  $X_o$ , corresponding to each particular process:

$$\frac{dX_T}{dT} = a + b X_o \quad (18-A)$$

where parameter  $a$  is the value of  $dX_T/dT$  for a hypothetical member of the homologous series with  $X_o = 0$  and parameter  $b$  coincides with the value of the second derivative ( $\partial^2 X_T / \partial T \partial X_o$ ). Since a process with no activation barrier is expected to remain so at all temperatures (for instance, a chemical reaction involving no bond breakage will show a zero activation energy irrespective of temperature), it can be concluded that for  $X_o = 0$  the derivative  $dX_T/dT$  must also be zero, thus implying that  $a = 0$ . Hence, from eqs 17-A and 18-A:

$$T_d = \frac{1}{b} = \text{constant} \quad (19-A)$$

Equations 17-A and 19-A are consistent with the hypothesis used above according to which the energy barrier of a process with  $X_o = 0$  is expected not to depend on temperature, and they imply that the higher the value of  $X_o$  for a particular process the higher the temperature dependence of its  $X_T$  value: along a certain homologous series, the members with the higher energy barriers will show  $X_T$  values more sensitive to temperature than the members with the lower energy barriers.

However, this argument should be considered only as an approximation to the real behavior of activated physico-chemical processes. For instance, it could have been assumed that the dependence given in eq 18-A can be described by a second degree polynomial ( $dX_T/dT = X_o/T_d = a + b X_o + c X_o^2$ ), the required condition  $a = 0$  leading then to  $T_d = 1/(b + c X_o)$ . Nevertheless, provided that the energy barrier range along the series is narrow enough, the quadratic term  $c X_o^2$  is expected to have a negligible contribution when compared with  $b X_o$ . Thus, although a certain dependence of  $T_d$  on  $X_o$  cannot be excluded, it is not a direct proportion relationship indeed. Therefore, if this conclusion is accepted, a simple inspection of eq 11-A reveals that the pre-exponential factor  $Y_\infty$  in eq 1 must be somehow correlated with the activation barrier  $X$  as a consequence of the temperature dependence of the latter (only a direct proportion relationship between parameters  $T_d$  and  $X_o$  would abolish that correlation).

Finally, because of the (at least partially) entropic nature of parameter  $A_X$ , its variation from one member of the series to another and, so, its interdependence with the value of  $X_o$ , cannot be discarded beforehand, and the potential effect that this variation (along with that of  $T_d$ ) may have on the profile of the  $X - \ln Y_\infty$  plots may be analyzed in detail with the aid of numerical simulations (see Section 8.1).

Although the argument so far developed in this section is of an eminently theoretical nature, a rather solid proof can be found from the experimental standpoint. As will be shown later (Table 2-A, Appendix 4), the three lowest values of parameter  $T_d$  (819, 1117 and 1309 K), among those calculated for 17 homologous reaction series, corresponded to chemical processes involving a protein as one of their reactants. Furthermore, the fourth lowest value (1416 K) corresponded to the reactions of biomimetic enzyme-like complexes with  $O_2$  to yield thermally labile peroxo species. Considering that proteins share the unusual feature of their structure being largely dependent on temperature (for instance, a gentle heating may be enough to result in the breaking of hydrogen bonds between residual amino acids), it seems indeed logical that the corresponding activation energies be more temperature dependent than usual (when the reactant structure is temperature independent). Since a low value of  $T_d$  means precisely that the activation energy is more sensitive to temperature than ordinary, it can be concluded that these results strongly support the physical model (dependence of the Arrhenius and Eyring parameters on temperature) as an explanation of the kinetic compensation effect.

### APPENDIX 3: Application to chemical kinetics: modified Eyring law

By derivation in the original version of the Eyring equation:

$$\frac{d(\ln k_T)}{dT} = \frac{1}{T} + \frac{\Delta H_{\neq}^{\circ}}{RT^2} \quad (20-A)$$

Assuming now that the activation enthalpy increases linearly with temperature:

$$\Delta H_{\neq,T}^{\circ} = \Delta H_{\neq,0}^{\circ} \left(1 + \frac{T}{T_d}\right) \quad (21-A)$$

Here  $\Delta H_{\neq,0}^{\circ}$  is the activation enthalpy at 0 K for a particular member of the reaction series and  $T_d$  the doubling temperature ( at which  $\Delta H_{\neq,T}^{\circ} = 2 \Delta H_{\neq,0}^{\circ}$  ). From equations 20-A and 21-A and posterior integration:

$$\frac{d(\ln k_T)}{dT} = \frac{1}{T} + \frac{\Delta H_{\neq,0}^{\circ}}{RT} \left( \frac{1}{T_d} + \frac{1}{T} \right) \quad (22-A)$$

$$\int d(\ln k_T) = \int \left[ \frac{1}{T} + \frac{\Delta H_{\neq,0}^{\circ}}{RT} \left( \frac{1}{T_d} + \frac{1}{T} \right) \right] dT \quad (23-A)$$

$$\ln k_T = \left(1 + \frac{\Delta H_{\neq,0}^{\circ}}{RT_d}\right) \ln T - \frac{\Delta H_{\neq,0}^{\circ}}{RT} + \ln A_H \quad (24-A)$$

where  $\ln A_H$  is the integration constant. This equation can also be written in its equivalent form (modified Eyring equation):

$$k_T = A_H T^{1 + \frac{\Delta H_{\neq,0}^{\circ}}{RT_d}} e^{-\frac{\Delta H_{\neq,0}^{\circ}}{RT}} \quad (25-A)$$

the relationship between the new pre-exponential factor ( $A_H$ ) and the activation entropy being then (from eqs 7, 21-A and 24-A):

$$A_H = \frac{k_B (c^{\circ})^{1-n}}{h} e^{\frac{\Delta S_{\neq}^{\circ}}{R}} (e T_m)^{-\frac{\Delta H_{\neq,0}^{\circ}}{RT_d}} \quad (26-A)$$



## APPENDIX 4: *Tabulated kinetic data*

$E_{a,2} - E_{a,1}$ [kJ mol <sup>-1</sup> ]	$T_m$ [K]	$k_1/k_2$ expected	$k_1/k_2$ found	Reference
9 ± 2	301	39.6	0.43	58
10 ± 2	298	66.4	2.58	59
17 ± 3	286	1.04 × 10 <sup>3</sup>	58.0	49
18 ± 6	286	1.63 × 10 <sup>3</sup>	3.90	60
20 ± 5	294	3.56 × 10 <sup>3</sup>	12.5	43
21 ± 7	298	4.06 × 10 <sup>3</sup>	0.80	59
22 ± 10	223	1.41 × 10 <sup>4</sup>	0.11	61
26 ± 1	306	2.28 × 10 <sup>4</sup>	1.71	62
27 ± 4	292	7.40 × 10 <sup>4</sup>	0.01	63
32 ± 3	408	1.33 × 10 <sup>4</sup>	12.8	64
32 ± 5	426	7.99 × 10 <sup>3</sup>	2.08	64
33 ± 2	296	5.81 × 10 <sup>5</sup>	169	65
38 ± 2	233	2.52 × 10 <sup>8</sup>	248	66
40 ± 3	268	7.41 × 10 <sup>7</sup>	2115	66
42 ± 8	301	2.20 × 10 <sup>7</sup>	75.5	67
75 ± 17	334	5.24 × 10 <sup>11</sup>	6.35	68
124 ± 30	419	3.00 × 10 <sup>15</sup>	109	64

(a)  $E_{a,1}$  and  $E_{a,2}$  are the lowest and highest activation energies for each reaction series, respectively.

(b)  $T_m$  is the experimental mean temperature for each reaction series.

(c)  $k_1 / k_2$  is the ratio between the highest and lowest rate constants at the temperature  $T_m$  for each reaction series.

(d) Expected ratio: calculated assuming the same Arrhenius pre-exponential factors for all the members of the series.

(e) Found ratio: experimentally observed value.

Table 1-A. Expected (non-compensated) and found (compensated) rate constant ratios at the mean experimental temperature for different homologous reaction series taken from the chemical literature.

$N$	$r$	$E$ [kJ mol <sup>-1</sup> ]	$E(k)$ [%]	$T_d$ [K]	$T_{ik,exp}$ [K]	$T_{ik,sim}$ [K]	Reference
4	0.955	3.31	33.3 ± 20.3	3121 ± 774	503 ± 110	476 ± 243	64
4	1.000	0.57	29.4 ± 5.5	2087 ± 35	355 ± 5	358 ± 5	68
5	0.976	3.33	23.1 ± 5.6	2873 ± 406	477 ± 62	521 ± 52	66
5	0.995	0.91	15.6 ± 6.2	2954 ± 203	479 ± 29	507 ± 22	64
5	0.999	0.02	0.6 ± 0.1	1309 ± 33	240 ± 5	239 ± 5	58
6	0.928	3.42	49.1 ± 13.2	1557 ± 373	277 ± 55	286 ± 151	62
6	0.988	0.55	9.3 ± 2.7	2200 ± 193	373 ± 29	408 ± 22	67
6	0.996	0.10	2.0 ± 0.4	2091 ± 109	357 ± 16	371 ± 14	60
8	0.987	1.43	22.7 ± 3.3	1117 ± 93	211 ± 14	195 ± 12	63
8	0.998	1.86	26.4 ± 4.3	2976 ± 87	482 ± 12	493 ± 11	64
9	0.978	2.29	21.6 ± 4.3	2517 ± 227	420 ± 34	477 ± 26	65
9	0.989	0.80	7.2 ± 1.1	2646 ± 167	440 ± 25	464 ± 22	43
10	0.837	4.00	61.4 ± 11.2	1416 ± 380	256 ± 59	245 ± 192	66
10	0.962	1.45	36.5 ± 7.0	819 ± 105	163 ± 16	137 ± 13	61
13	0.810	1.50	22.1 ± 9.2	1436 ± 379	259 ± 57	273 ± 234	59
13	0.964	0.75	3.0 ± 0.4	3887 ± 346	627 ± 52	681 ± 45	49
13	0.990	0.53	31.3 ± 8.5	1655 ± 84	292 ± 13	294 ± 49	59

- (a)  $N$  is the number of reactions in each homologous series.  
(b)  $r$  is the correlation coefficient of the experimental enthalpy-entropy linear plot.  
(c)  $E$  is the experimental activation enthalpy fitting error.  
(d)  $E(k)$  is the random error percentage of the rate constants according to the simulations.  
(e)  $T_d$  is the calculated doubling temperature for each reaction series.  
(f)  $T_{ik,exp}$  and  $T_{ik,sim}$  are the experimental and simulated (most probable) isokinetic temperatures for each reaction series, respectively.

Table 2-A. Experimental and simulated kinetic data for different homologous reaction series taken from the chemical literature.